Thesis for the Degree of Master of Engineering

Fluorene-based Polymer and Oligomer Electrolytes for Polymer Solar Cells

by

Mutia Anissa Marsya

Department of Polymer Engineering

The Graduate School

Pukyong National University

August, 2017

Fluorene-based Polymer and Oligomer Electrolytes for Polymer Solar Cells

Advisor: Prof. Joo Hyun Kim

by
Mutia Anissa Marsya

A thesis submitted in partial fulfillment of the requirements for the degree of

Master of Engineering

in Department of Polymer Engineering, The Graduate School, Pukyong National University

August, 2017

Fluorene-based Polymer and Oligomer Electrolytes for Polymer Solar Cells

A dissertation

by

Mutia Anissa Marsya

Approved by :

(Chairman) Prof. Mun Ho Kim

(Member) Prof. Seong Il Yoo

(Member) Prof. Joo Hyun Kim

Contents

List of figures

List of Tables

List of Schemes

Fluorene-based Polymer and Oligomer Electrolytes for Polymer Solar Cells

Mutia Anissa Marsya

Departement of Polymer Engineering, The Graduate School

Pukyong National University

Abstract

A series fluorene-based conjugated polymer, poly[6,6'-(2-(thiophen-2-yl)-9H-fluorene-9,9-diyl)bis(N,N,N-trimethylhexan-1-aminium) bromide] **(PFT Salt)**, poly[6,6'-(2-phenyl-9H-fluorene-9,9-diyl)bis(N,N,N-trimethylhexan-1-aminium) bromide] **(PFB Salt)**, poly[9,9-bis(6-(3,5-bis(bromomethyl)phenoxy) hexyl)-2,7-dibromo-9H-fluorene-thiophene] **(P[IsoPh-OH-T])**, poly[1,1',1",1'"-(((2-(thiophen-2-yl)-9H-fluorene-9,9-diyl)bis(hexane-6,1-diyl))bis (benzene-5,3,1-triyl)) tetrakis (N,N,N-trimethylmethanaminium) bromide] **(P[IsoPh-Br-T] Salt)**, and oligomer, 6,6',6",6'"-(phenyl-2,5-diylbis(9H-fluorene-9,9,2-triyl))tetrakis(N,N,N-trimethyl-hexan-1-aminium) bromide **(FBF Salt)**, 6,6',6",6'"-(thiophene-2,5-diylbis(9H-fluorene-9,9,2-triyl))tetrakis(N,N,N-trimethylhexan-1-aminium) bromide **(FTF Salt)**, 6,6'-(2,7-diphenyl-9H-fluorene-9,9-diyl) bis(N,N,N-trimethylhexan-1-aminium) bromide **(BFB Salt)**, 6,6'-(2,7-di(thiophen-2-yl)-9H-fluorene-9,9-diyl) bis(N,N,N-trimethylhexan-1-aminium) bromide **(TFT Salt)**, 6,6'-(2,7-bis(2,4-difluorophenyl)-9H-fluorene-9,9-diyl)bis(N,N,N-trimethylhexan-1-aminium) bromide **(Bf-F-Bf Salt)** has been synthesized and utilized as cathode interfacial layer in inverted polymer solar cell. Cathode interfacial layer (CIL) or usually known as electron transfer layer (ETL) is interpretative to improving the power conversion efficiency (PCE) and long-term stability of an organic photovoltaic cell that utilizes a high work function cathode. The KPM result that the polymers: PFt salt, PFB salt, P-IsoPh-Br-T salt, P-IsoPh-OH-T, and the oligomers, demonstrates a strong impact on the interfacial

interaction to the electrode by reducing the work function of ITO. To investigate the effect of CIL on the photovoltaic properties, inverted type PSCs with a device configuration of ITO/ZnO/CIL/PTB7-$PC_{71}BM/MoO_3$/Ag were fabricated. Maximum power conversion efficiency (PCE) of the PSCs based on polyfluorene is showed up to 7.91% from the device based PFB salt and for the oligomer is showed up to 8.26% from the device based BfFBf salt. Nevertheless all the result indicate that fluorene-based conjugated electrolytes are excellent CIL materials for polymer solar cells.

Fluorene-based Polymer and Oligomer Electrolytes for Polymer Solar Cells

Mutia Anissa Marsya

Departement of Polymer Engineering, The Graduate School

Pukyong National University

Abstract

Fluorene 기반 공액 고분자 (PFT salt, PFB salt, P-IsoPh-OH, and P-IsoPh-Br salt) 및 올리고머 (FTF salt, FBF salt, TFT salt, BFB salt and BfFBf salt) 가 합성되어 IPSC 의 Cathode 계면 층으로 이용되고 있다. Cathode 계면 층 (CIL) 또는 일반적으로 electron transfer layer (ETL)로 불리는 cathode interfacial layer (CIL)는 높은 일함수를 가진 Cathode 을 사용한 PSC 의 power conversion efficiency (PCE)와 장기(Long-term) 안정성을 향상시키는 것으로 보인다. KPM 결과는 고분자와 올리고머가 ITO 의 일 함수를 감소시켜 전극과의 계면 상호 작용에 강한 영향을 미친다는 것을 보여줍니다. CIL 이 광전지 특성에 미치는 영향을 알아보기 위해 ITO / ZnO / CIL / PTB7-$PC_{71}BM$ / MoO_3 / Ag 의 장치 구성을 갖는 역전형 PSC 를 제작 하였다. Polyfluorene 기초한 PSC 의 최대 전력 변환 효율 (PCE)은 장치 기반 PFB salt 으로부터 7.91 %까지 나타났고, 올리고머는 장치 기반 BfFBf salt 으로부터 8.26 %까지 나타났다. 그럼에도 불구하고 모든 결과는 fluorene 기반의 공액 전해질이 고분자 태양 전지에 우수한 CIL 물질이라는 것을 보여줍니다.

Chapter I. Introduction

I-1. Introduction to organic solar cells

The globalization era was totally consuming high energy than before. The demand for energy is accelerating at the high rate due to the fast growth of developing nations and the emergence of new economies. Oil still remained the world's leading fuel, accounting for 32.9% of global energy consumption [1]. The continuous burning of fossil fuels not only give a serious problem to the climate but also is an unsustainable method of energy production. In contrast, the photovoltaic/ solar cells could convert the sunlight into electricity and have the potential to cleanly and sustainably meet future energy demands.

The first practical solar cell was developed in April 1954 at Bell Laboratory [2]. It was inorganic solar cell based on silicon (Si). In the past 20 years, the demand for solar energy has grown consistently with growth rates of 20–25% per year, reaching 427 MW in 2002[3]. Commercial solar cells are typically fabricated using inorganic materials. These days, the organic materials were successfully invented and give interesting performance solar cell due to they're easy fabrication. Organic solar cell (OSCs) devices

are based on organic semiconductors carbon-based materials. The main backbones are comprised of alternating C–C and C=C bonds. OSCs approach commercial efficiencies of around 3 % whereas commercial inorganic solar cells (ISCs) are over 15%, thus the efficiency of OSCs must be improved in order to compete with ISCs [4].

The development organic solar cells to improve the performance could be done by material design and morphology optimization of the photoactive layer. The power conversion efficiency (PCE) for bulk-heterojunction (blended OSC) have achieved over 11%[5-12]. Despite recent improvements in performance, device stability still remains a challenge for commercialization of this technology.

I-2. The operating principle of an organic solar cell

The organic solar cells device can convert the light become a charge electricity by following the exciton dissociation process[13]. The majority of the organic solar cells device have a

planar layered structure, where the organic active layer that can absorb the light sandwiched between the two electrodes. One of them must be transparent and usually indium tin oxide (ITO) used as transparent conductive oxide (TCO), because it allows producing better results. The other electrode is very often aluminum for conventional device and silver or gold are often used in the inverted solar cells device.

The organic semiconductors such as molecule polymers, oligomers, dendrimers, etc. all are based on conjugated π electron system. A conjugated system is a system of connected π-orbitals with delocalized electrons. The crucial property related to this conjugation are that the π electrons are easier to move freely than σ electrons. Therefore by absorption of energy the π bonds system breaks creating excitons or free charges. Molecular π-π* orbitals correspond to the Highest Occupied Molecular Orbital (HOMO) and Lowest Unoccupied Molecular Orbital (LUMO)[14].

The generation of electricity from the sunlight using solar cells consists of different successive event. Further, the mechanism is explained in detail.

I-2-1 Absorption of light and exciton generation

Organic compounds show interesting optical and electrical properties due to the presence of conjugated π electron system. Organic materials with large absorption coefficients in the order of 10^5/cm are quite common[15]. The bandgap or bond energy in organic semiconductors is tuned with the energy of solar spectrum. When light absorbed, the π-bonds system breaks forming an exciton. The band gaps of OSCs range from 1.7 to 3.0 eV and must be chosen wisely to ensure adequate exciton generation[16-18].

I-2-2. Exciton diffusion

The photogenerated excitons are characterized by a very small lifetime of few picoseconds limiting the mobility of excitons to a few polymer units or molecules. Excitons must be formed and disassociated to generate a current. The structure of the organic cells includes a component that corresponds to an electron donor and a component that corresponds to an electron acceptor. There is an interface between those two components where the excitons must reach in order to disassociate. The critical condition for an efficient organic solar cell is the fact that the exciton can diffuse a

pretty large distance within its lifetime. If the interface on average is 10 nanometers from where the exciton is generated, but during its lifetime the exciton only diffuses 5 nanometers, no current will be produced. In other words, during its lifetime, the exciton must be able to diffuse and reach the interface between the donor and acceptor components. If a system is designed with large diffusion lengths and the migration of the exciton takes too long, then the average distance between where the exciton is generated and the interface can be reduced.

I-2-3. Exciton dissociation

Exciton dissociation refers to the process of splitting the electrostatically coupled electron-hole pair into free charges. The dissociation of excitons happens at the donor-acceptor interfaces. The electron acceptor (A) is the material with larger HOMO and LUMO and the one with smaller HOMO and LUMO level will act as the electron donor (D). When the gap in HOMO and in LUMO is not acceptable, the exciton may hop without charge separation. To reach the efficient charge separation we need:

$$\Delta(LUMO_D\text{-}LUMO_A) > \text{Exciton energy.}$$

I-2-4. Charge transport and charge collection

Once the excitons have disassociated into two separated species, the electron and the hole, they must move efficiently toward the electrodes. The charges can recombine during the way to the electrode, mainly if the same material serves as the transport medium for both carriers' type. The efficiency of separation depends on how fast the electrons and the holes can move away from each other.

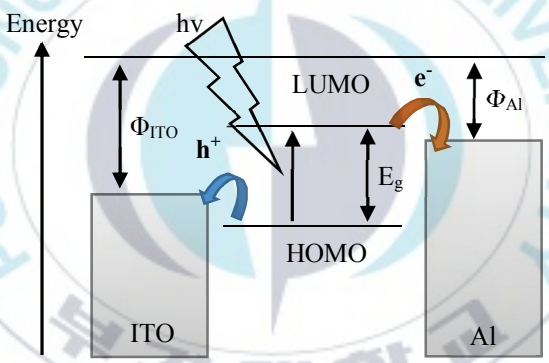

Figure I-1. Energy levels and light harvesting. Under the light radiation from the sun, an electron is promoted to the LUMO leaving a hole behind in the HOMO. The Al electrode will collect the electron and the holes will be transferred to the ITO electrode. F: work function, E_g: optical bandgap.

I-3. Interfacial layer

Conventional OSC device architecture consists of a bulk heterojunction (BHJ) active layer sandwiched between a transparent conducting electrode, such as indium tin oxide (ITO) glass, and a low-work-function metal electrode (which usually uses the Al material). The BHJ active layer is achieved by a blend of the p-type polymer donor and n-type fullerene acceptor materials dissolved in common solvent, and subsequent phase segregation results in the formation of two interpenetrated percolated networks during the annealing process after spin-coating[19]. In such active layers, only excitons formed within a distance of ~20 nm from the p-type polymer donor/n-type fullerene derivative acceptor interface can reach the interface and then dissociate into free charge carriers[20-22]. In order to achieve good performances, however, it is mandatory that a BHJ comprises an interfacial layer between the active layer and both electrode to facilitating transport of the electron and the hole to strike the electrode.

The electrode interfacial layer divided by anode interface layer and cathode interface layer. The holes flow to the anode

electrode via anode interface layer so it usually called hole transfer layer (HTL), while the electrons flow to the cathode via cathode interface layer then the name is electron transfer layer (ETL).

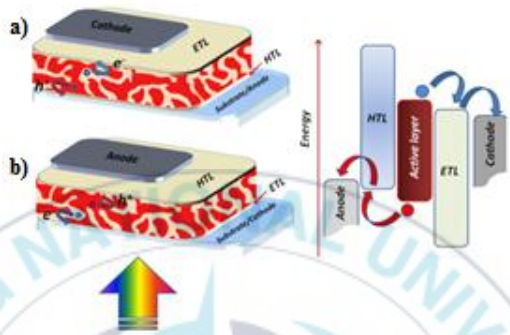

Figure I-2. a) Standard geometry for bulk heterojunction (BHJ) device; and b) an inverted BHJ device [23]

I-3-1. Anode interface layer/ HTL

The major function of anode interface layer or hole transporting layer are the following:

a) The HTL have much higher charge transporting properties compared with the active materials, the charges that reach the interfaces with the HTL/ETL can quickly move away from the active layer. This is an efficient way to avoid charge recombination.

b) The HTL can efficiently blocked electrons and it can avoid leak currents.

c) The HTL can protect the anode electrode from traditional corrosive. This guarantees an improved stability and longer lifetime of the devices[24].

I-3-1-1. Poly (3,4-ethylenedioxythiophene) polystyrene sulfonate (PEDOT:PSS)

PEDOT:PSS is polymer mixture of two ionomers. One component is made up of sodium polystyrene sulfonate which is a sulfonated polystyrene. The sulfonyl groups are deprotonated and carry a negative charge. The other component poly(3,4-ethylenedioxythiophene) or PEDOT is a conjugated polymer and carries positive charges and is based on polythiophene. Together the charged macromolecules form a macromolecular salt[25]. PEDOT:PSS is the most widely used HTL in standard geometry BHJ solar cells, due to its high work function (matching the HOMO level of commonly used donor polymers well), high transparency in the visible range (higher than 80%), good electrical

conductivity and the ability to reduce the ITO surface roughness[26], while increasing its work function.

The influence of HTL physical properties and thermal annealing process on device performance using four distinct formulations of PEDOT:PSS have been studied by P. G. Karagiannidis and team. They demonstrated that vertical distribution of active layer was correlated with HTL surface free energy. Hydrophilic surface of PSS leads to separation of surface and significant recombination losses were observed after pre-annealing. The decrease in surface free energy of HTL together with the reduction of series resistance could improve the device performance[27].

I-3-1-2. Metal Oxide (Mox)

Metal oxides (MOs) are the most abundant materials in the Earth's crust and are ingredients in traditional ceramics. MO semiconductors are strikingly di□erent from conventional inorganic semiconductors such as silicon and III–V compounds with respect to materials design concepts, electronic structure, charge transport mechanisms, defect states, thin-film processing

and optoelectronic properties, thereby enabling both conventional and completely new functions[28]. However, in OSCs, despite the progress towards a better adhesion of PEDOT:PSS on top of organic layers, the acidic/hygroscopic nature of the compound is still detrimental for the top-side metal electrode. Its hygroscopic nature can easily absorb the water and it becomes corrosive due to the acidic nature (pH ranging from 1.5 to 2.5) of PEDOT:PSS[29]. To substitute PEDOT:PSS, few transition metal oxide have been synthesized and characterized. The most typical ones are MoO_3, WO_3, V_2O_5, and NiO[30-34]. These metal oxides reveal good hole transportation ability. In addition, the large band gap of the metal oxides achieves good electron blocking properties.

I-3-2. Cathode interface layer/ ETL

The electron transport layer (ETL) is a layer which has a high electron affinity and high electron mobility. These characteristics allow electrons to flow across the layer, while holes are “blocked” and cannot go through. The insertion of cathode interface layers can form ohmic contacts at both electrodes, which minimizes the energy barrier and benefits efficient charge carrier

transport and extraction[35-37]. The ETL also could help prevent damage to the active layer during thermal evaporation of the metal cathode. That's benefit can increase the intrinsic stability of the device by minimizing degradation which affects the active layer.

I-3-2-1. Zinc Oxide (ZnO)

ZnO is a wide bandgap semiconductor of the II-VI semiconductor group. The native doping of the semiconductor due to oxygen vacancies or zinc interstitials is n-type[38]. There is several materials which have been investigated as optimum ETL like titanium sub-oxide (TiOx)[39], several polymers, such as hydrophilic conjugated 2,7-carba-zole- 1,4-phenylene alternating copolymers PCP-NOH or PCP-EP, poly(ethyleneimine) (PEI)[40] and conjugated polyelectrolyte poly- [(9,9-bis(30-(N,N-dimethylamino)propyl)-2,7-fluorene)-alt-2,7-(9,9-ioctylfluorene)] (PFN)[41] and PFPA[42]. Among the materials mentioned above, ZnO is the most extensively investigated one for ETLs in the inverted OSCs, mainly due to its suitable energy levels, high electron mobility, good transparency, environmental stability and low cost.

The energy levels of ZnO (conduction band bottom and valence band top) are at around 4.4 eV and 7.8 eV, respectively. Such band positions allow ZnO to function well for electron collection and hole blocking. The relatively high electron mobility of ZnO makes it a suitable material for cathode interface layers to reduce the charge recombination. The good transparency in the whole visible spectrum benefits in lowering the optical loss and the band edge cut-off of ZnO at around 375 nm can block UV light and accordingly protect the organic materials from photodegradation under UV light irradiation. [43]

I-3-2-3. Water/alcohol soluble conjugated polymers (WSCPs)

The water/alcohol soluble conjugated polymer (WSCPs) materials have been studied as alternatives the metal oxide, ZnO, as ETLs in OSCs. These materials have been successfully used as the interlayer materials in optoelectronic devices due to their many unique advantages. They are usually processed from environmentally friendly solvents (such as alcohol), which is important for future industrial applications and can offer

orthogonal solvent processability to prevent the solvent erosion problem during multilayer device fabrication. [44]

Generally, WSCPs are a kind of polymers that contain π-conjugated/ non- conjugated main chains and the side chains are modified with highly polar pendant groups (such as ammonium groups, sulfonate groups, phosphonate groups etc.) which can increase their solubility in water and polar organic solvents such as methanol. Many groups have demonstrated that the use of alcohol-/water-soluble polymers as cathode interfacial layers can effectively enhance the efficiency of organic solar cells, such as poly(ethylene oxide) (PEO),[45-46] polyethyleneimine ethoxylated (PEIE) and polyethyleneimine (PEI),[47] (WPF-oxy-F) and (WPF-6-oxy-F).[48-49]

I-3-2-4. Fluorene Derivatives

Interest in fluorene-based organic semiconductors has increased to their ability to display high levels of the (polarized) photo- and electroluminescence as well as useful electronic charge-transport properties.[50-52] Both, oligo- and polyfluorene derivatives have been studied extensively and they properties have

been found to display superior characteristics, such as significantly improved optoelectronic behavior (e.g., field-effect mobility, photoluminescence, circular dichroism, and photovoltaic performance),[53–56] as well as, for instance, the ability to form oriented fibers.[57–58]

Luo and his team (2009) was the first invented fluorene derivatives as an interlayer to the solar cell. They apply alcohol/water soluble conjugated polymers based on fluorene inspired by the success of applying that material in the PLEDs[59]. Poly[(9,9-bis{3′-[(N,N-dimethyl)-N–ethylammonium]propyl}-2,7-fluorine)-,7- (9,9-dioctylfluorene)-co-(4,7,-dithien-2-yl)-2,1,3-benzotiadiazole] dibromide (PFNBr-DBT15) and poly[(9,9-bis(3′-(N,N-dimethylamino) propyl)-2,7-fluorene)-alt-1,4-phenylene] dibromide (PFPNBr) were synthesized and characterized with enhanced open-circuit voltage which lead to better of PCE of polymer solar cells. He *et al.* (2012) has recently reported that an inverted solar cell with poly [(9,9-bis (3′- (N, N-dimethylamino) propyl) -2,7-fluorene) -alt-2,7-(9,9–dioctyl-fluorene)] (PFN) as the cathode interfacial layer achieved high power conversion efficiency about 9.2%, with a simple

device structure. The devices based on PFN show superior performance over the ZnO-based devices (9.15% versus 8.35%).[41]

Chapter II. Polyfluorene-based electrolytes as an interfacial layer of inverted polymer solar cells.

II-1. Introduction

Polymer solar cells (PSCs) with a blend of polymer and fullerene derivation as an active layer have caught much attention because of their potential application to convert the solar radiation by fabricating large-scale printing, flexible device and low-cost solution processing[7-9]. There is two main types device structure of PSCs, the conventional structure (ITO/HTL/active layer/ETL/metal electrode) and the inverted structure (ITO/ETL/active layer/HTL/metal electrode). In the conventional structure, the instability comes from the HTL material PEDOT:PSS which is corrosive to the ITO and the presence of oxygen and moisture because the device usually sandwiched between ITO and the low work function metal (normally Ca/Al), which are very easily oxidized in the air[60]. The inverted structure becomes superior because their increase the stability by using air-stable metal as the anode (such as Ag and Au). The problem was

the ITO have high work function caused the collecting of the electron from the fullerene acceptor not efficient. Therefore, in order to improve the power conversion efficiency (PCE) of the inverted structure, the solution processed organic interlayer between ITO and active layer become an important issue.

As we know the amazing performance of simple inverted polymer solar cells have been invented by introducing PFN as cathode interfacial layer (see Chapter I). The research on the cathode interface material still attracted the researcher by modifying the backbone, pendant group, different counter ion, and self-assembled conjugated polyelectrolytes. In this chapter, we synthesized polymer electrolytes based on fluorene. We used quaternarization reaction to produce quarter ammonium salt of the polymer[60].

II-2. Experimental

II-2-1. Material and Synthesis

II-2-1-1. Materials

Methylene chloride (MC) was distilled over CaH_2. Toluene was bubbling with nitrogen. All other chemicals were purchased from

Sigma-Aldrich co, Alfa Aesar (A Johnson Matthey Company) or Toyo Chemical Industry (TCI) and were used as received unless otherwise described.

II-2-1-2. Synthesis

II-2-1-2-1. General procedure of Suzuki coupling polymerization reaction

A mixture of aryl bromide, aryl boronic ester, 5.0 mol % of tetrakis(triphenylphosphine) palladium [$Pd(PPh_3)_4$] and several drops of aliquat336 in degassed 1:1 (by volume) mixed solvent of toluene and 2M K_2CO_3 aqueous was stirred for 12 hours at 80 ^oC under the N_2 atmosphere. The mixture allowed to cool to room temperature and precipitated by dropping on methanol (150 ml).

II-2-1-2-2. General procedure of Stille coupling polymerization reaction

A mixture of aryl bromide, tin compound, tri (O-tolyl)phosphine, and 5.0 mol % of bis(dibenzylideneacetone)palladium(0) [$Pd(dba)_2$] in toluene/DMF was stirred for 10-15 minutes at

110 ºC under N_2 atmosphere. The mixture allowed to cool to room temperature and precipitated by dropping on methanol (150 ml).

II-2-1-2-3. Synthesis of 2,7-dibromo-9,9-bis-(6-bromo-hexyl)-9H-fluorene (2)

A mixture of compound 2,7-dibromo-9H-fluorene (16.20 g, 50.00 mmol), 1,6-dibromo-hexane (152.23 ml, 1 mol), 30 mL of 2M KOH solution in water and 5.0 mol % of PTC (0.693 g, 0.250 mmol) was stirred for 18 hours at 80 ºC under N_2 atmosphere. A portion of 100 mL of water has added the mixture and allowed to cool to room temperature. The mixture was extracted with methylene chloride (MC) and the extracted organic layer was dried over anhydrous $MgSO_4$. The organic solvent was removed by using a rotary evaporator. The excess of 1,6-dibromo-hexane was recovered by vacuum distillation. The crude product was purified by column chromatography on silica gel using MC/n-hexane and recrystallization using methanol to get very pure of the product. The yield of white solid was 25.35 g (78.3%). ^{1}H-NMR (400 MHz, $CDCl_3$, ppm): δ 7.52 (s, 1H), 7.48~7.47 (d, J=1.8 Hz, 1H), 7.44~7.43 (d, J=1.5 Hz, 1H), 3.32~3.28 (t, J=6.8, 2H) 1.95~1.90

(m, 2H), 1.71~1.64 (m, 2H), 1.24~1.16 (m, 2H), 1.12~1.05 (m, 2H), 0.62~0.53 (m, 4H). ^{13}C NMR (151 MHz, $CDCl_3$, ppm) δ 152.24, 139.15, 130.42, 126.16, 122.03, 121.34, 55.64, 40.15, 34.03, 32.83, 29.04, 27.86, 23.54.

II-2-1-2-4. Synthesis of poly[2-[9,9-Bis-(6-bromo-hexyl)-9H-fluoren-2-yl]-thiophene] (PFT)

This polymer PFT was synthesized by Stille coupling polymerization reaction. The 2,5-Bis-tributylstannanyl-thiophene (0.4 mmol), the 2,7-Dibromo-9,9-bis-(6-bromo-hexyl)-9H-fluorene (2) (0.4 mmol) and Tri(O-tolyl)phosphine (50% mol, 76 mg, 0.2 mmol) were mixed in degassed Toluene. Bis(dibenzylideneacetone) palladium(0) [$Pd(dba)_2$] (11,5 mg) were added to the mixture as catalyst. The reaction mixture was stirred and heated to reflux for 20 minutes under N_2 atmosphere. Then the reaction mixture was cooled to room temperature, and the polymer was precipitated by addition of methanol (150 mL), filtered through a Soxhlet thimble. The precipitate was then subjected to Soxhlet extraction with methanol, hexanes, and chloroform. The polymer was recovered as solid from the

chloroform fraction by precipitation from methanol. ^{1}H-NMR (400 MHz, $CDCl_3$, ppm): δ 7.74~7.68 (m, 3H), 7.61~7.57 (m, 2H), 7.52~7.30 (m, 3H), 3.31~3.27 (m, 4H), 2.08~1.98 (m, 4H), 1.69~1.62 (m, 4H), 1.26~1.22 (m, 4H), 1.13~1.11 (m, 4H), 0.95~0.73 (m, 4H).

II-2-1-2-5. Synthesis of poly[2-[9,9-bis-(6-bromo-hexyl)-9H-fluoren-2-yl]-benzene] (PFB)

This polymer PFB was synthesized by Suzuki coupling reaction. The benzene boronic ester (4) (0.132 gr, 0.4 mmol), the 2,7-Dibromo-9,9-bis-(6-bromo-hexyl)-9H-fluorene (2) (0.26 gr, 0.4 mmol), 7% mol of tetrakis(triphenylphosphine) palladium [Pd(PPh3)4] (0.032 g, 0.028 mmol), and several drops of aliquat. 336 in 6 mL of degassed 1:1 (by volume) mixed solvent of Toluene and 2M K_2CO_3 aqueous was stirred for 72 hours at 110 ^{o}C under the N_2. Then the reaction mixture was cooled to room temperature, and the polymer was precipitated by addition of methanol (150 mL). To remove the catalyst the precipitate was then dissolved in chloroform and add 50 ml of ammonia water for overnight. To the mixture was added water (50 mL) and chloroform (50 mL). The

chloroform layer was separated, washed with water (50 mL X 2), dried over magnesium sulfate, and concentrated. The polymer was recovered as solid by adding 1 ml of THF to the concentrated polymer and make precipitate in methanol. ^{1}H-NMR (400 MHz, $CDCl_3$, ppm): δ 7.74~7.68 (m, 3H), 7.62~7.57 (m, 2H), 7.52~7.30 (m, 3H), 3.31~3.27 (m, 4H), 2.08~1.99 (m, 4H), 1.69~1.62 (m, 4H), 1.26~1.22 (m, 4H), 1.13~1.12 (m, 4H), 0.95~0.73 (m, 4H).

II-2-1-2-6. Synthesis of poly[6,6'-(2-(thiophen-2-yl)-9H-fluorene-9,9-diyl)bis(N,N,N-trimethylhexan-1-aminium) bromide] (PFT Salt)

Poly fluorene – thiophene polyelectrolyte was synthesized by combining 30 mg of Poly[2-[9,9-Bis-(6-bromo-hexyl)-9H-fluoren-2-yl]-thiophene] (PFT) with 6 mg trimethylamine in THF at reflux temperature for 48 h, then the solvent was removed. The polyelectrolytes were dried in vacuum overnight and obtained as an orange solid.

II-2-1-2-7. Synthesis of poly[6,6'-(2-phenyl-9H-fluorene-9,9-diyl)bis(N,N,N-trimethylhexan-1-aminium) bromide] (PFB Salt)

Polyfluorene – Benzene polyelectrolyte was synthesized by combining 30 mg of Poly[2-[9,9-Bis-(6-bromo-hexyl)-9H-fluoren-2-yl]-benzene] (PFB**)** with 6 mg trimethylamine in THF for 6 days, then the solvent was removed. The polyelectrolytes were dried in vacuum overnight and obtained as a gray solid.

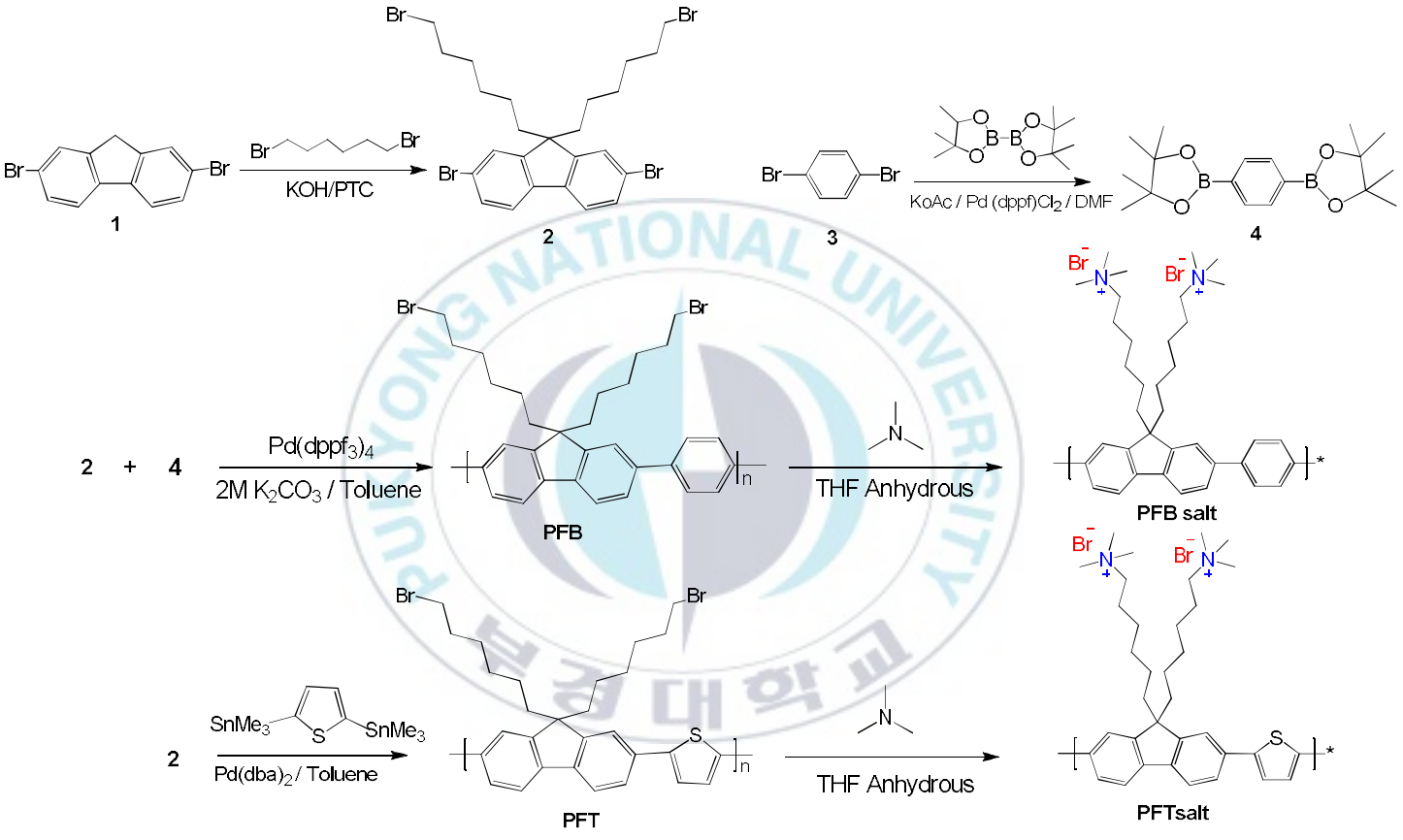

Scheme II-1. Synthesis of Conjugated Polymer Electrolytes

II-2-2. Fabrication of PSCs

In order to fabricate the inverted type organic photovoltaic (OPV) with the device structure: [ITO/ZnO (40 nm)/ ETL (~ 5 nm)/active layer (PTB7:$PC_{71}BM$, 100 nm)/MoO_3 (10 nm)/Ag (100 nm)], a ZnO layer was deposited on an ITO substrate by the sol-gel process. A thin film of ZnO sol-gel precursor was cured at 200 °C for 10 min. A thin layer of interlayer material was prepared by spin coating with a MeOH solution of oligomer compound (1 mg/mL) at 4000~5000 rpm for 60 seconds onto the ITO or ZnO. The typical thickness of a cathode buffer layer was less than 5 nm at room temperature. The active layer was spin-cast from a mixture of PTB7 and $PC_{71}BM$ (obtained by dissolving 10 mg of PTB7 and 15 mg of $PC_{71}BM$ in 1 mL of chlorobenzene with 3% (w/v) 1,8-diiodooctane (DIO)) and stirring at 2000 rpm for 120 s. The active solution was then filtered through a 0.2 m membrane filter δ before spin coating. Successive layers of MoO_3 and Ag were thermally evaporated through a shadow mask, with a device area 13 mm^2 at 2 x 10^{-6} Torr.

II-2-3. Measurement

Synthesized compounds were characterized by ^{1}H and ^{13}C NMR spectra, and it was recorded on a JEOL JNM ECP-400 spectrometer. The elemental MASS analysis of synthesized compounds was carried out on an Elementar Vario macro/micro elemental analyzer, Shimadzu GC-MS QP-5050A spectrometer and Perkin-Elmer Voyager- DE PRO. UV-Visible spectra were recorded using UV-Vis spectrophotometer (JASCO V-530). Cyclic voltammetry (CV) was performed by an Ivium B14406 with a three-electrode cell in a solution of 0.10 M tetrabutylammonium hexafluorophosphate (Bu_4NPF_6) in acetonitrile anhydrous at a scan rate of 100 mV/s. Pt coil and wire were used as the counter and working electrode, respectively. An Ag/Ag^{+} electrode was used as the reference electrode. Prior to each measurement, the cell was deoxygenated with nitrogen. Elemental analysis was performed using X-ray photoelectron spectroscopy (XPS) (Thermo VG Scientific (UK), MultiLab2000) and recorded using Al Kα X-ray line (15 kV, 300 W). Kelvin probe microscopy (KPM) measurements (KP Technology Ltd. Model KP020) were performed on the ZnO layers, with and without ETL, and the work

function of the samples were estimated by measuring the contact potential difference between the sample and the KPM tip. The KPM tip was calibrated against a standard reference gold surface, with a work function of 5.1 eV. A thin film of ETL was prepared by spin coating it on ITO/ZnO surface, using a methanol (MeOH) solution (1 mg/mL) of the electron transport materials at the ambient condition to measure the contact potential difference using KPM and investigate the effective work function of the interlayer coated substrate. The current density–voltage measurements were performed under simulated light (AM 1.5G, 1.0 sun condition/100 mW/cm^2) from a 150 W Xe lamp, using a KEITHLEY Model 2400 source measure unit. A calibrated Si reference cell with a KG5 filter certified by National Institute of Advanced Industrial Science and Technology was used to confirm 1.0 sun condition.

II-3. Result and discussion

II-3-1. XPS elemental analysis

The quarter ammonium salt of the polymer was confirmed by XPS elemental analysis (Figure II-1). We confirmed that the quaternization reaction was succeeded, prove by the N 1s peak appeared (at ~400 eV) in the polymers salt. For the polymers before quaternization reaction, N 1s peaks cannot be observed.

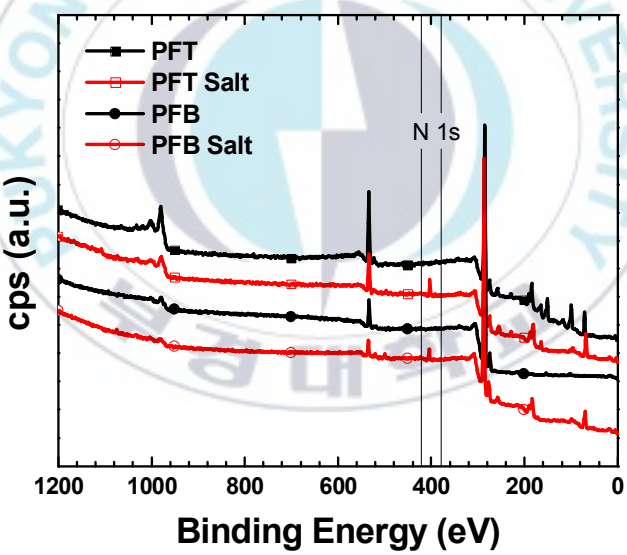

Figure II-1. Survey X-ray photoelectron spectra of PFT and PFB before and after quaternization reaction.

II-3-2. Optical and electrochemical properties

Figure II-2 (a) show of the UV-visible spectra of the polymer before quaternization reaction in chloroform solution and in thin film, while (b) show the UV-visible spectra of the polymer after quaternization reaction in methanol solution and in a thin film. Both PFT and PFB exhibit the similar features at before and after quaternization reaction, the absorption spectra of PFT, PFB, PFT salt and PFB salt peak 440, 369, 446, and 358 nm in the film; 434, 358, 441, 345 nm in solution, respectively. The films exhibit red-shift absorption bands because in the solid state, the π-conjugated backbone length was enlarged that can induce intense intramolecular packing[61].

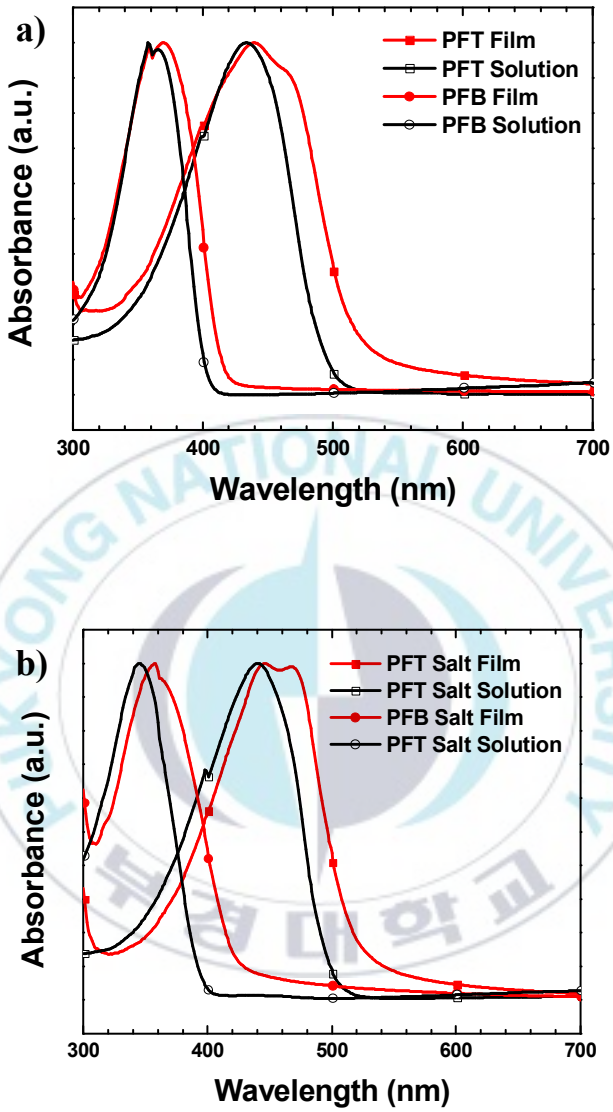

Figure II-2. UV-Visible spectra of PFT and PFB in chloroform solution and thin film (a); and their quaternary ammonium salt, PFT salt and PFB salt in methanol solution and thin film (b).

Figure II-3 corresponding to PL emission of the polymer before (a) and after (b) quaternization reaction. The PL emission peak of PFT, PFB, PFT salt and PFB salt are 502, 419, 550, and 424 nm in the film; 474, 411, 506, and 405 in nm solution. All thin films spectra exhibit broadened and red-shifted PL bands peak due to molecular aggregation in the film state.

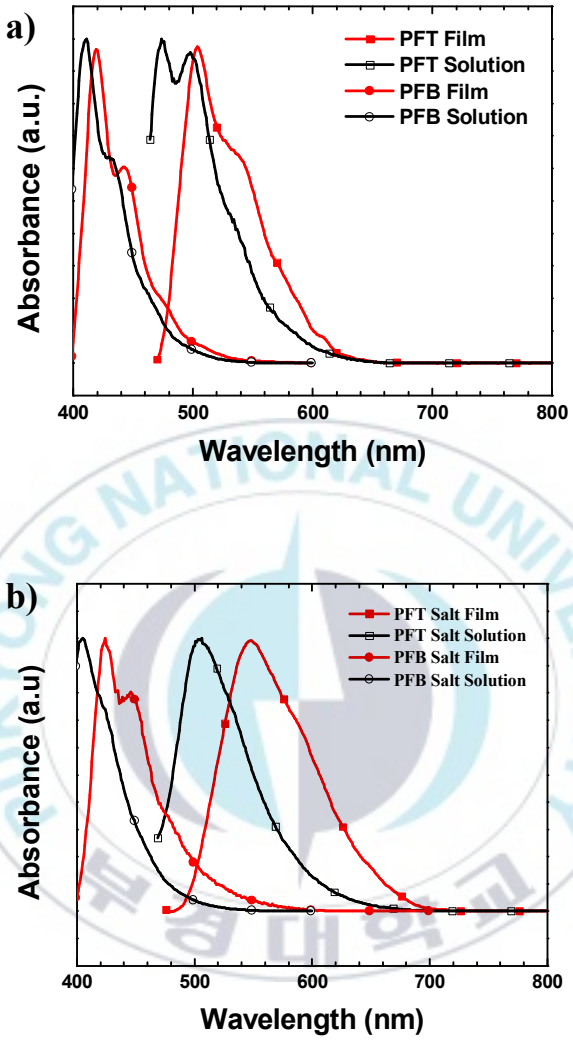

Figure II-3. Photoluminescence (PL) spectra of PFT and PFB in chloroform solution and thin film (a); and their quaternary ammonium salt, PFT salt and PFB salt in methanol solution and thin film (b).

The electrochemical properties of the polymer were investigated by cyclic voltammetry (CV) using tetra-n-butylammoniumhexafluorophosphate (n-Bu_4NPF_6, 0.1 M in acetonitrile) as the supporting electrolyte with a glass carbon working electrode, a platinum wire counter electrode, and an Ag/AgCl electrode as the reference electrode. The onset voltage of oxidation process for PFT and PFB were determined at 0.73 V and 0.93 V, respectively (Figure II-4). The reference electrode was calibrated by the ferrocene/ferrocenium (Fc/Fc^+) and the onset potential was 0.35 V (absolute energy of Fc/Fc^+ was 4.8 eV below the vacuum level)[62] to obtain accurate energy levels. The HOMO and LUMO levels could be calculated as E_{LUMO} =-e(E_{re} + 4.45) (eV) and E_{HOMO} = -e(E_{ox}+4.45) (eV).[63] Table II-1 presented the summary of optical and electrochemical properties data.

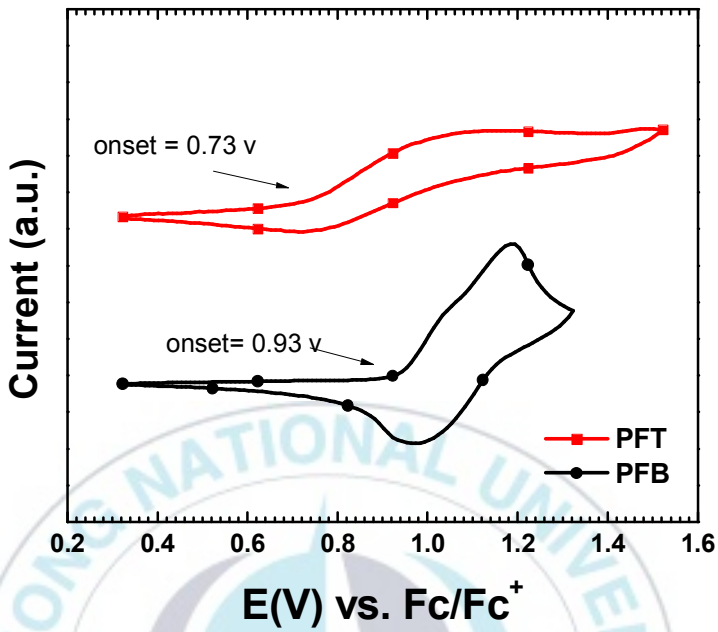

Figure II-4. Cyclic voltammogram of PFT and PFB as films measured in 0.1 M Bu_4NPF_6 in acetonitrile.

Table II-1. Summary of optical and electrochemical properties data of polymer.

Polymer	UV-vis absorption spectra		Photoluminescence Spectra		Cyclic Voltammetry		E_g^{opt}
	solution	film	solution	film	HOMO	LUMO	
	λ_{max}/nm	λ_{max}/nm	λ_{max}/nm	λ_{max}/nm	(eV)	(eV)	(eV)
PFT	434	440	474	502	-5.18	-3.27	2.82
PFB	358	369	411	419	-5.38	-3.25	3.36
PFT Salt	441	446	506	550	-	-	2.78
PFB Salt	345	358	405	424	-	-	3.46

II-3-3. Interfacial properties

In order to evaluate the interface interaction between polymer salt and ITO or ZnO, Kelvin Probe Microscopy (KPM) was used to calculate the effective work function (WF). The WF of bare ITO is 5 eV, whereas the ITO/PFT Salt and ITO/PFB Salt reduce the work function of ITO by 0.87 eV and 1.05 eV, respectively. We also measure with pristine ZnO (the WF bare ZnO is 4.4 eV) and both of the ZnO/PFT Salt, ZnO/PFT Salt can reduce the WF of ZnO by 0.25 eV (Figure II-5). However, the WF decreased after being modified by polymer salts indicates the formation of a favorable interface dipole which can lower the Schottky barrier and facilitate charge injection.[64]

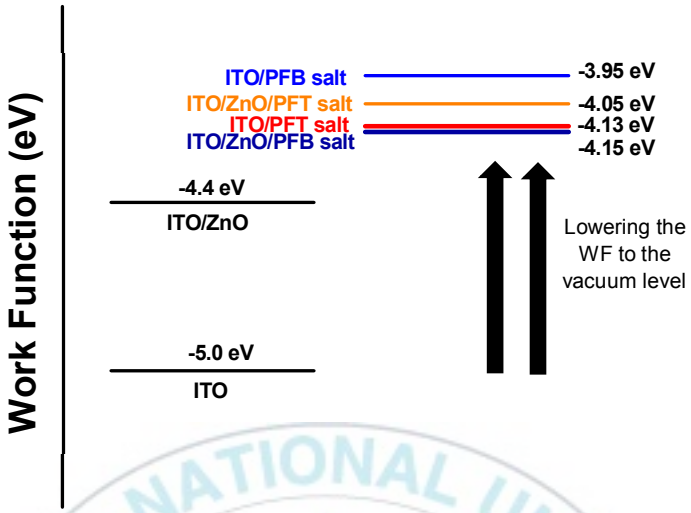

Figure II-5. Work function data from a matrix of the ITO electrodes coated with PF-X salt and ZnO/PF-X salt film.

II-3-4. Photovoltaic properties

OSC was fabricated using polymer salt as cathode interfacial layer (CIL). It was demonstrated that methanol treatment can improve the surface properties of ZnO films due to possible hydrogen bonding interactions.[65] Therefore, devices with methanol treatment were also fabricated as a reference. The current density (J) – voltage (V) curves of OSCs under AM 1.5G simulated

illumination with intensity of 100 mW/cm^2 are shown in Figure II-6 and the corresponding short-circuit currents (J_{sc}), open-circuit voltages (V_{oc}), fill factors (FF) and power conversion efficiencies (PCE) are summarized in Table II-2.

The device with **PFT salt** showed an open circuit voltage (V_{OC}) of 0.74 V, a short circuit current (J_{SC}) of 15.30 mA/cm^2, a fill factor (FF) of 69.2 % and a PCE of 7.83 %. The device with **PFB salt** gave a V_{OC} of 0.74 V, a J_{SC} of 15.28 mA/cm^2, a FF of 69.9 and a PCE of 7.91%. As shown in Table II-2, all device with CIL have better performance compared to the device treated with methanol (MeOH). The slight improvement of PCE occurred due to the better contact between the active layer and the metal cathode. The enhanced J_{sc} contributed by the reduced work function for better energy alignment.[66] **PFB salt** exhibit higher PCE (7.91% vs 7.83%) than **PFT salt.** That result is related with KPM result that PFB salt performs better to decrease the WF of the metal electrode than PFT salt.

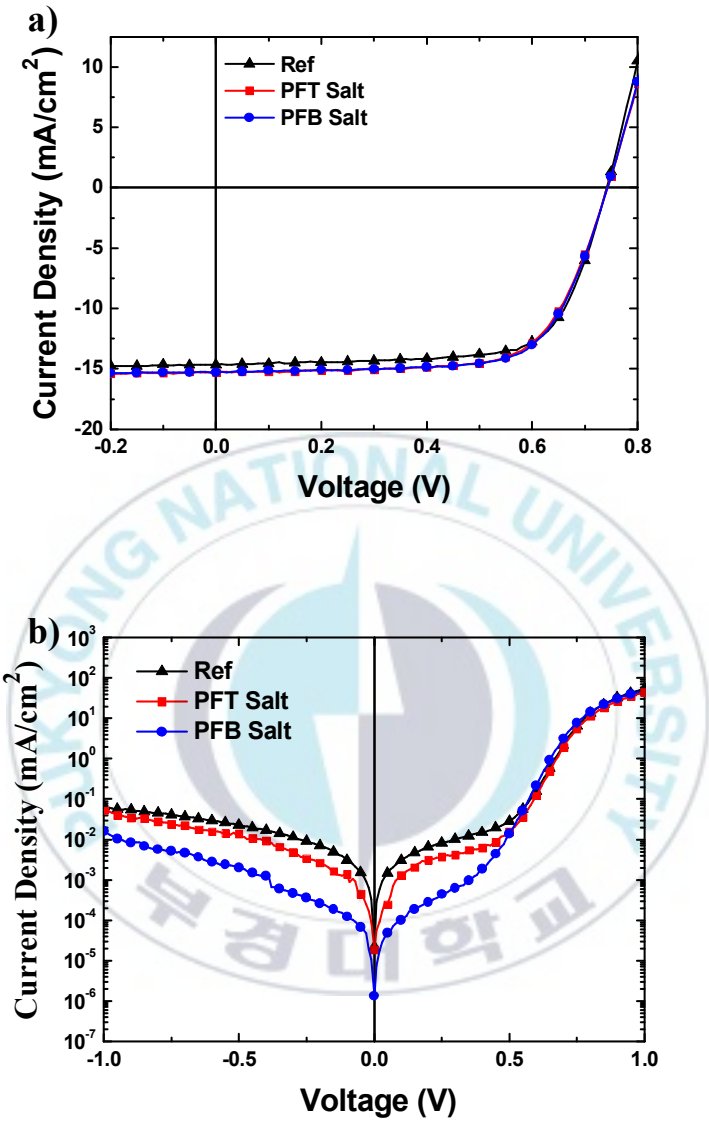

Figure II-6. Current density–voltage curves of polymer salts under AM 1.5G simulated illumination with an intensity of 100 mW/cm^2 (a) and under the dark condition (b).

Table II-2. Photovoltaic performance of PTB7:$PC_{71}BM$-based PSCs with interlayer and methanol treatment.

Sample Name	Jsc (mA/cm^2)	Voc (V)	FF (%)	PCE (%)
ZnO/MeOH	14.65 (14.55)	0.74 (0.74)	71.6 (71.1)	7.66 (7.66)
ZnO/PFT Salt	15.30 (15.25)	0.74 (0.74)	69.2 (68.55)	7.83 (7.73)
ZnO/PFB Salt	15.28 (15.23)	0.74 (0.74)	69.9 (69.4)	7.91 (7.81)

The averages for the photovoltaic parameters of each device are given in parentheses.

II-4. Conclusion

The polyfluorene-based electrolytes, PFB salt and PFT salt were synthesized and developed as cathode interfacial materials. XPS studies showed that the quaternization reaction of all polymer was succeeded. The work function of the metal electrode was decreased by all polymer salt which leads to better energy alignment for electron transport. All polymer salt deposited as cathode interface layer in inverted polymer solar cells and exhibit a good performance by enhancing the PCE of the device. **PFB salt** has higher PCE than **PFT salt**, correlate with the performance of **PFB salt** that can lower the WF of metal electrode better than **PFT salt**.

Chapter III. Alcohol-soluble conjugated polymer as interfacial layer of inverted polymer solar cells

III-1. Introduction

In the previous chapter, we successfully introduced the polymer salt based on fluorene. To further research for enhancing the performance of solar cells, in this chapter we present the new materials for ETL by increasing the amount of pendant, quaternary ammonium salt ($N^+ Br^-$). However, these electrolytes usually have movable positive and negative ions, which can travel easily into the active layer, thus possible reason to determine the effect of a number of pendants group to the performance of the PSCs. Isophthalate was attached to the fluorene monomer and the final conversion polymer produced four pendants in each fluorene.

III-2. Experimental

III-2-1. Material and synthesis

III-2-1-1. Materials

Methylene chloride (MC) was distilled over CaH_2. Toluene was bubbling with nitrogen. All other chemicals were purchased from Sigma-Aldrich co, Alfa Aesar (A Johnson Matthey Company) or Toyo Chemical Industry (TCI) and were used as received unless otherwise described.

III-2-1-2. Synthesis

III-2-1-2-1. General Procedure of Stille coupling polymerization reaction

The stille coupling polymerization in this chapter is followed by the method of polymerization reaction (II-2-1-2-1) in chapter II.

III-2-1-2-2. Synthesis of 2,7-dibromo-9,9-bis-(6-bromo-hexyl)-9H-fluorene (1)

A mixture of compound 2,7-dibromo-9H-fluorene (16.20 g, 50.00 mmol), 1,6-Dibromo-hexane (152.23 ml, 1 mol), 30 mL of 2M

KOH solution in water and 5.0 mol % of PTC (0.693 g, 0.250 mmol) was stirred for 18 hours at 80 °C under N_2 atmosphere. A portion of 100 mL of water has added the mixture and allowed to cool to room temperature. The mixture was extracted with methylene chloride (MC) and the extracted organic layer was dried over anhydrous $MgSO_4$. The organic solvent was removed by using a rotary evaporator. The excess of 1,6-Dibromo-hexane was recovered by vacuum distillation. The crude product was purified by column chromatography on silica gel using MC/n-hexane and recrystallization using methanol to get very pure of the product. The yield of white solid was 25.35 g (78.3%). ^{1}H-NMR (400 MHz, $CDCl_3$, ppm): δ 7.5200 (s, 1H), 7.4779~7.4733 (d, J=1.8 Hz, 1H), 7.44~7.43 (d, J=1.5 Hz, 1H), 3.32~3.28 (t, J=6.8, 2H) 1.94~1.90 (m, 2H), 1.71~1.64 (m, 2H), 1.24~1.16 (m, 2H), 1.128~1.05 (m, 2H), 0.62~0.53 (m, 4H). ^{13}C NMR (151 MHz, $CDCl_3$, ppm) δ 152.24, 139.15, 130.42, 126.16, 122.03, 121.34, 55.64, 40.15, 34.03, 32.83, 29.04, 27.86, 23.54.

III-2-1-2-3. Synthesis of tetramethyl 5,5'-(((2,7-dibromo-9H-fluorene-9,9-diyl)bis(hexane-6,1-diyl))bis(oxy))diisophthalate (2)

A mixture of compound 1 (9.75 g, 15.00 mmol), Dimethyl 5-hydroxyisophthalate (7.25 g, 34.5 mmol), K_2CO_3 (11.74 g, 85 mmol) and 20.0 mol % of 18-crown-6 (0.792 g, 3 mmol) in 30 ml acetonitrile was stirred for 24 hours at 80 °C under N_2 atmosphere. A portion of 100 mL of water was added the mixture and allowed to cool to room temperature. The mixture was extracted with ethyl acetate (EA) and the extracted organic layer was dried over anhydrous $MgSO_4$. The organic solvent was removed by using a rotary evaporator. The crude product was purified by column chromatography on silica gel using EA/n-hexane. The yield of white sticky liquid was 8.23 g (60.4%). ^{1}H-NMR (400 MHz, $CDCl_3$, ppm): 8.24~8.24 (t, *J*= 3.65 Hz, 1H), 7.74~7.73 (d, *J*= 3.6 Hz, 1H), 7.51 (s, 1H), 7.47~7.46 (d, *J*= 3.7, 1H), 7.45~7.45 (d, *J*= 4.5, 2H), 3.94 (s, 2H), 3.49 (s, 6H), 1.97~1.93 (m, 2H), 1.66~1.59 (m, 2H), 1.29~1.20 (m, 2H), 1.18~1.10 (m, 2H), 0.66~0.58 (m, 2H). ^{13}C NMR (151 MHz, $CDCl_3$, ppm) δ 165.88, 157.22, 150.00,

140.09, 133, 51, 130.59, 129.63, 122.53, 121.44, 118.40, 68.71, 51.49, 43.87, 30.22, 29.60, 25.86, 24.39.

III-2-1-2-4. Synthesis of ((((2,7-dibromo-9H-fluorene-9,9-diyl)bis(hexane-6,1-diyl))bis(oxy))bis(benzene-5,3,1-triyl))tetramethanol (3)

Lithium Aluminum Hydrate ($LiAlH_4$) (0.57 g, 15 mmol) was under vacuum to remove the moisture in the reaction flask for 15 minutes. Anhydrous THF (30 ml) was added to dissolve $LiAlH_4$. Compound 2 (2.72 g, 3 mmol) was dissolved in anhydrous THF before injected to the reaction flask. And the reaction was stirred for 24 hours at room temperature under N_2 atmosphere. A portion of 100 mL of water has added the mixture and allowed to cool to room temperature. Dilute HCl was added to neutralize the mixture. The mixture was extracted with ethyl acetate (EA) and the extracted organic layer was dried over anhydrous $MgSO_4$. The organic solvent was removed by using a rotary evaporator. The crude product was purified by column chromatography on silica gel using EA/n-hexane and recrystallization using methylene chloride to get very pure of the product. The yield of white powder was 1.91

g (80%). ^{1}H-NMR (400 MHz, $CDCl_3$, ppm): 7.6503~7.6301 (d, *J*= 20.2 Hz, 1H), 7.56~7.56(d, *J*= 3.6 Hz, 1H), 7.49~7.47 (dd, J_1= 20.15 Hz, J_2= 4.5 Hz, 1H), 6.89~6.87 (d, *J*= 16.5, 1H), 6.76 (s, 2H), 3.86~3.82 (t, *J*= 16 Hz, 2H), 2.05~2.01 (t, *J*= 20.15 Hz, 2H), 1.56~1.51 (m, 2H), 1.29 (s, 2H), 1.26~1.19 (m, 2H), 1.15~1.08 (m, 2H), 0.61~0.53 (m, 2H). ^{13}C NMR (151 MHz, $CDCl_3$, ppm) δ 146.71, 134.16, 125.15, 121.25, 119.63, 115.79, 92.21, 81.46, 68.21, 52.74, 33.45, 29.55, 27.53, 26.01, 17.78.

III-2-1-2-5. Synthesis of 9,9-bis(6-(3,5-bis(bromomethyl)phenoxy)hexyl)-2,7-dibromo-9H-fluorene (4)

The compound 4 (1.03 g, 1.3 mmol) was dissolved in 10 ml of distillate MC in the two neck RB flask. To the flask, phosphorus tribromide (PBr_3) (0.3 ml, 2.6 mmol) was added slowly using dropping funnel. Wash the dropping funnel with distillate MC to make sure the PBr_3 was added completely to the flask. The reaction was stirred for 24 hours at room temperature. A portion of 100 mL of water has added the mixture and allowed to cool to room temperature. Potassium carbonate (K_2CO_3) solution 2M was added to neutralize the mixture. The mixture was extracted with

methylene chloride (MC) and the extracted organic layer was dried over anhydrous $MgSO_4$. The organic solvent was removed by using a rotary evaporator. The crude product was purified by column chromatography on silica gel using MC/n-hexane. The yield of white sticky powder was 0.83 g (80%). ^{1}H-NMR (600 MHz, $CDCl_3$, ppm): δ 7.55~7.51 (m, 2H), 7.48~7.44 (m, 4H), 6.97 (s, 2H), 6.81 (s, 2H), 4.41 (s, 4H), 3.86~3.81 (t, J = 6.4 Hz, 2H), 1.99~1.91 (m, 2H), 1.63~1.56 (m, 2H), 1.25~1.18 (dd, J = 14.9, 7.7 Hz, 2H), 1.17~1.08 (m, 2H), 0.66~0.56 (m, 2H). ^{13}C NMR (151 MHz, $CDCl_3$, ppm) δ 159.57, 152.38, 139.56, 130.32, 126.31, 121.72, 121.37, 115.29, 68.05, 55.72, 40.22, 32.99, 29.64, 29.17, 25.85, 23.56.

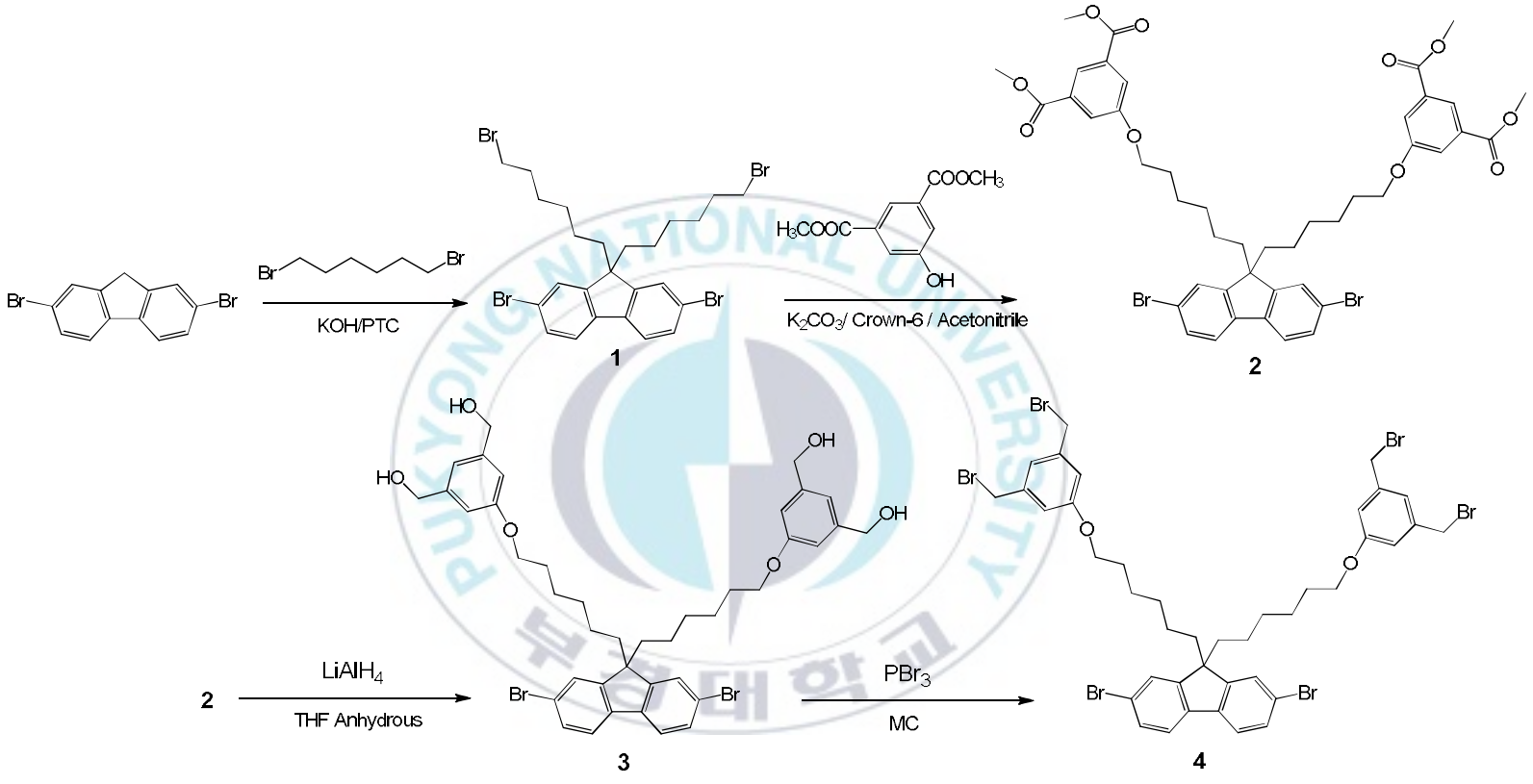

Scheme III-1. Synthesis of conjugated monomer based on IsoPhthalate

III-2-1-2-6. Synthesis of poly((((2,7-dibromo-9H-fluorene-9,9-diyl)bis(hexane-6,1-diyl))bis(oxy))bis(benzene-5,3,1-triyl))tetramethanol-thiophene (P[IsoPh-OH-T])

This polymer P[IsoPh-OH-T] was synthesized by stille coupling reaction. The reaction following the same method with general procedure of stille coupling polymerization reaction above. The 2,5-bis-trimeythylstannyl-thiophene (0.081 gr, 0.2 mmol), compound 3 (0.159 gr, 0.2 mmol) and tri(O-tolyl)phosphine (50% mol, 0.03 gr, 0.1 mmol) were mixed in degassed DMF. Bis(dibenzylideneacetone)palladium(0) [$Pd(dba)_2$] (5% mol, 6 mg, 0.01 mmol) were added to the mixture as catalyst. The polymer was precipitated by addition of deionized water (150 mL). ^{1}H-NMR (400 MHz, $CDCl_3$, ppm): 7.54~7.43 (d, *J*= 20.2 Hz, 1H), 7.40~7.40 (d, *J*= 10.6 Hz, 1H), 7.35~7.29 (t, *J*= 14.5 Hz, 1H), 6.89~6.87 (d, *J*= 16.5, 1H), 6.76 (s, 2H), 4.61 (s, 8H) 3.88~3.84 (t, *J*= 15 Hz, 2H), 3.65 (s, 4H) 2.05~2.01 (t, *J*= 20.15 Hz, 2H), 1.57~1.53 (m, 2H), 1.25~1.19 (m, 2H), 1.15~1.09 (m, 2H), 0.61~0.53 (m, 2H).

III-2-1-2-7. Synthesis of poly[9,9-bis(6-(3,5-bis(bromomethyl)phenoxy) hexyl)-2,7-dibromo-9H-fluorene-thiophene] (P[IsoPh-Br-T])

This polymer P[IsoPh-Br-T] was synthesized by Stille coupling reaction. The reaction following the same method with general procedure of stille coupling polymerization reaction above. The 2,5-bis-trimeythylstannyl-thiophene (0.164 gr, 0.4 mmol), compound 4 (0.419 gr, 0.2 mmol) and tri(O-tolyl)phosphine (50% mol, 0.06 gr, 0.2 mmol) were mixed in degassed Toluene. Bis(dibenzylideneacetone)palladium(0) [$Pd(dba)_2$] (5% mol, 12 mg, 0.02 mmol) were added to the mixture as catalyst. The polymer was precipitated by addition of methanol (150 mL). ^{1}H-NMR (400 MHz, $CDCl_3$, ppm): 7.52~7.52 (d, *J*= 17.8 Hz, 1H), 7.49~7.45 (d, *J*= 15.5 Hz, 2H), 6.95 (s, 1H) 6.85~6.79 (m, 2H), 4.40 (s, 8H), 3.84~3.82 (t, *J*= 10.05 Hz, 2H), 1.95~1.93 (t, *J*= 18.15 Hz 2H), 1.61~1.56 (m, 2H), 1.26~1.19 (m, 2H), 1.15~1.10 (m, 2H), 0.64~0.58 (m, 2H).

III-2-1-2-8. Synthesis of poly[1,1',1'',1'''-(((2-(thiophen-2-yl)-9H-fluorene-9,9-diyl)bis(hexane-6,1-diyl))bis(benzene-5,3,1-triyl))tetrakis(N,N,N-trimethylmethanaminium) bromide] (P[IsoPh-Br-T] Salt)

The poly[IsoPh-Br-T] electrolytes was synthesized by combining 30 mg of Poly[9,9-bis(6-(3,5-bis (bromomethyl) phenoxy) hexyl)-2,7- dibromo- 9H-fluorene-thiophene] (P[IsoPh-Br-T]**)** with 6 mg trimethylamine in anhydrous THF at reflux temperature for 6 days, followed by extraction with hexane using centrifuge. The hexane was then removed under reduced pressure. The polymer was dried in vacuum overnight and was obtained as an orange solid.

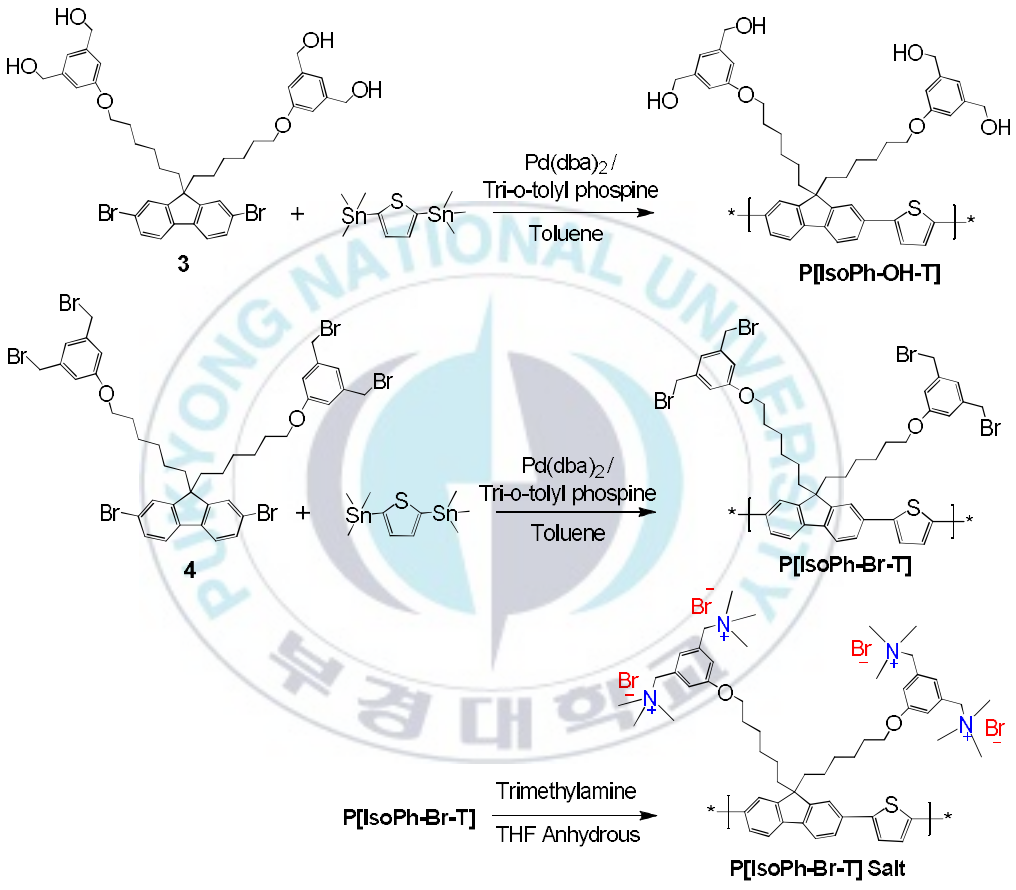

Scheme III-2. Synthesis of conjugated polymer based on IsoPhthalate

III-2-2. Fabrication of PSCs

In order to fabricate the inverted type organic photovoltaic (OPV) with the device structure: [ITO/ZnO (40 nm)/ ETL (~ 5 nm)/active layer (PTB7:$PC_{71}BM$, 100 nm)/MoO_3 (10 nm)/Ag (100 nm)], a ZnO layer was deposited on an ITO substrate by the sol-gel process. A thin film of ZnO sol-gel precursor was cured at 200 °C for 10 min. A thin layer of interlayer material was prepared by spin coating with a MeOH solution of oligomer compound (1 mg/mL) at 4000~5000 rpm for 60 seconds onto the ITO or ZnO. The typical thickness of a cathode buffer layer was less than 5 nm at room temperature. The active layer was spin-cast from a mixture of PTB7 and $PC_{71}BM$ (obtained by dissolving 10 mg of PTB7 and 15 mg of $PC_{71}BM$ in 1 mL of chlorobenzene with 3% (w/v) 1,8-diiodooctane (DIO)) and stirring at 2000 rpm for 120 s. The active solution was then filtered through a 0.2 m membrane filter δ before spin coating. Successive layers of MoO_3 and Ag were thermally evaporated through a shadow mask, with a device area 13 mm^2 at 2 x 10^{-6} Torr.

III-2-3. Measurement

Synthesized compounds were characterized by ^{1}H and ^{13}C NMR spectra, and it was recorded on a JEOL JNM ECP-400 spectrometer. The elemental MASS analysis of synthesized compounds was carried out on an Elementar Vario macro/micro elemental analyzer, Shimadzu GC-MS QP-5050A spectrometer and Perkin-Elmer Voyager- DE PRO. UV-Visible spectra were recorded using UV-Vis spectrophotometer (JASCO V-530). Cyclic voltammetry (CV) was performed by a Ivium B14406 with a three-electrode cell in a solution of 0.10 M tetrabutylammonium hexafluorophosphate (Bu_4NPF_6) in acetonitrile anhydrous at a scan rate of 100 mV/s. Pt coil and wire were used as the counter and working electrode, respectively. An Ag/Ag^{+} electrode was used as the reference electrode. Prior to each measurement, the cell was deoxygenated with nitrogen. Elemental analysis was performed using X-ray photoelectron spectroscopy (XPS) (Thermo VG Scientific (UK), MultiLab2000) and recorded using Al Kα X-ray line (15 kV, 300 W). Kelvin probe microscopy (KPM) measurements (KP Technology Ltd. Model KP020) were performed on the ZnO layers, with and without **ETL**, and the work

function of the samples were estimated by measuring the contact potential difference between the sample and the KPM tip. The KPM tip was calibrated against a standard reference gold surface, with a work function of 5.1 eV. The current density–voltage measurements were performed under simulated light (AM 1.5G, 1.0 sun condition/100 mW/cm^2) from a 150 W Xe lamp, using a KEITHLEY Model 2400 source measure unit. A calibrated Si reference cell with a KG5 filter certified by National Institute of Advanced Industrial Science and Technology was used to confirm 1.0 sun condition.

III-3. Result and Discussion

III-3-1. XPS elemental analysis

To support our assumption of the quaternization reaction is succeed, the X-ray photoelectron spectra (XPS) was carried out to analyze the chemical structure of P-IsoPh-Br-T salt and P-IsoPh-Br-T. Figure III-1 shows the N 1s peak appeared in the P-IsoPh-Br-T salt spectra. The binding energy of N 1s peak is 401.63 eV which only obtained in the quaterammonium salt that means the conversion reaction was succeeded.

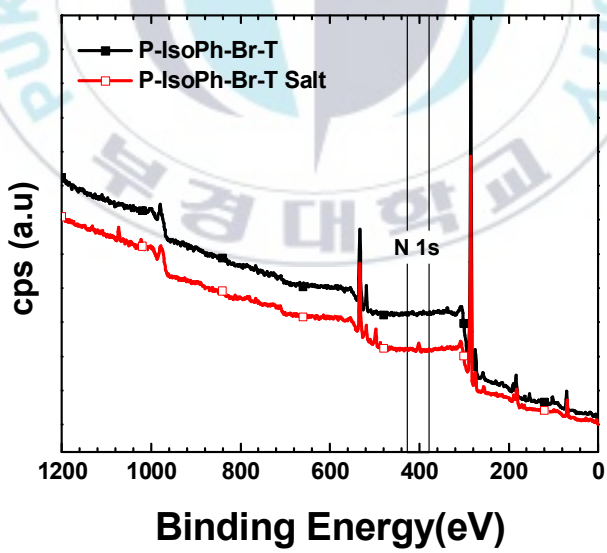

Figure III-1. Survey X-ray photoelectron spectra of P-IsoPh-Br-T and P-IsoPh-Br-T salt

III-3-2. Optical and electrochemical properties

Figure III-2 shows the normalized UV-Vis absorption and photoluminescence (PL) spectra for dilute methanol solutions and spin-coated thin films of P-IsoPh-Br-T (before and after quaternarization) and P-IsoPh-OH-T. The wavelength of the polymer solution absorptions bands peak at 280 nm for P-IsoPh-Br-T salt which is almost same with neutral compound (279 nm). Interestingly, the absorption peak of P-IsoPh-OH-T appeared at a longer wavelength, 471 nm in a solution state. In the thin film, P-IsoPh-Br-T salt peaks show red-shifted absorption to 298 nm and P-IsoPh-OH-T peaks show much broader at 473 nm. The corresponding solution PL bands peak at 500 nm for P-IsoPh-Br-T salt and 543 nm for P-IsoPh-OH-T. In the film state, the emission of P-IsoPh-Br-T salt shifted to a longer wavelength of 564 nm then P-IsoPh-OH-T peak of 545 nm.

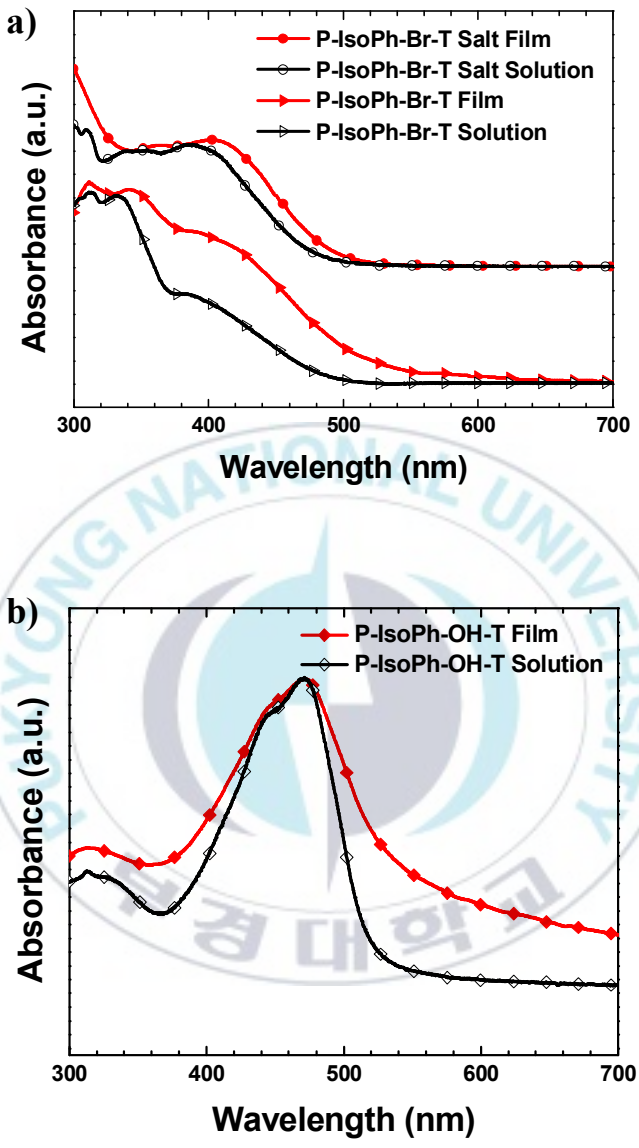

Figure III-2. UV-Visible spectra of P-IsoPh-Br-T in chloroform solution and thin film; P-IsoPh-Br-T salt (a) and P-IsoPh-OH-T in methanol solution and thin film (b).

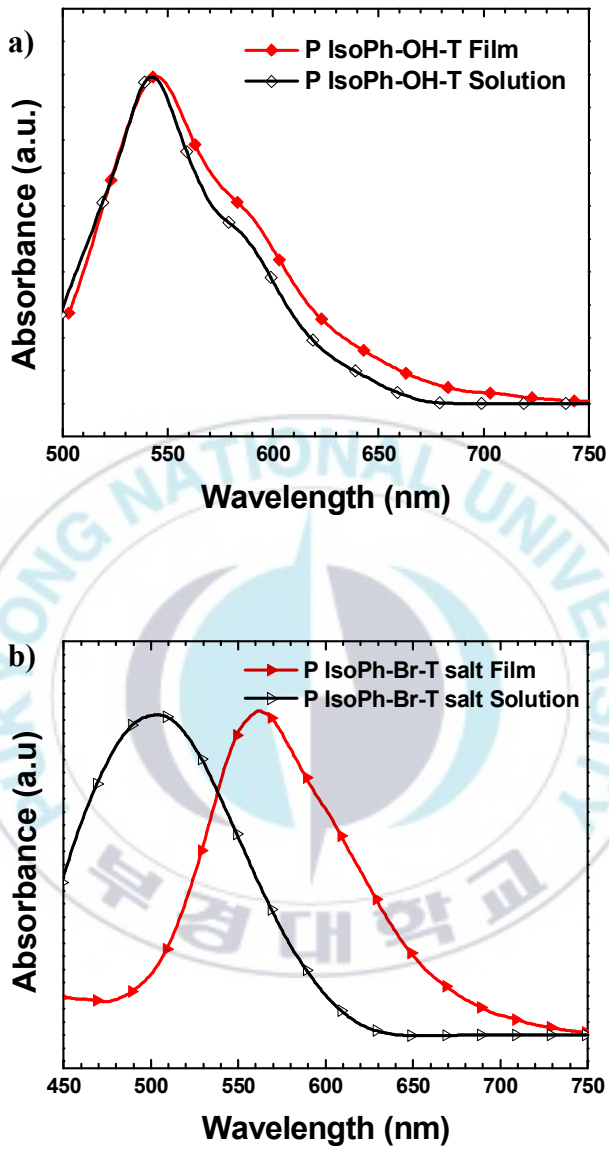

Figure III-3. Photoluminescence spectra of P-IsoPh-Br-T salt (a) and P-IsoPh-OH-T (b) in methanol solution and thin film.

The energy levels of the resulting polymer were determined by cyclic voltammetry (CV) using tetra-n-butylammoniumhexafluorophosphate (n-Bu_4NPF_6, 0.1 M in acetonitrile) as the supporting electrolyte with a glass carbon working electrode, a platinum wire counter electrode, and an Ag/AgCl electrode as the reference electrode. The CV curve is presented in Figure III-3. The onset voltages of oxidation process for P-IsoPh-Br-T and P-IsoPh-OH-T were observed to be 1.43 eV and 0.75 eV, respectively. The HOMO energy levels of both polymers were thus calculated to be 6.23 eV for P-IsoPh-Br-T and 5.55 eV for P-IsoPh-OH-T, using the ferrocene value of 4.8 eV below the vacuum as the internal standard.[62] The two molecules have deep HOMO level which beneficial to hole blocking ability with respect to various donor materials.[67] Table III-1 presented the summary of optical and electrochemical properties data.

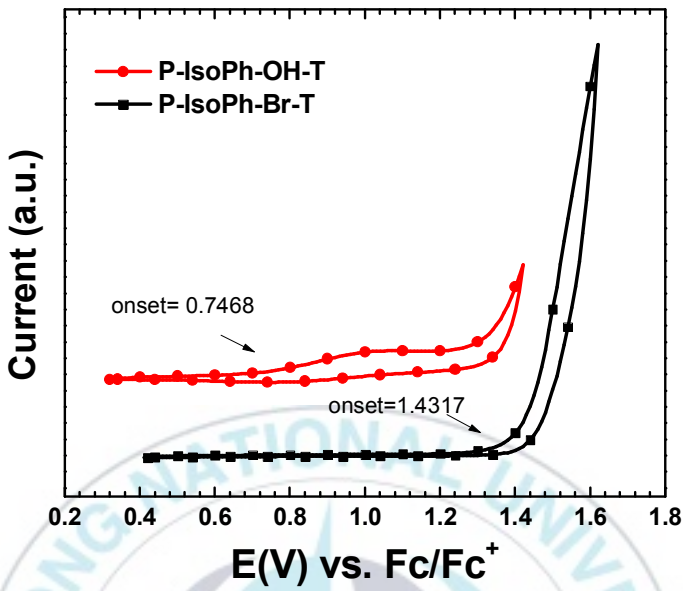

Figure III-4. Cyclic voltammograms of P-IsoPh-Br-T and P-IsoPh-OH-T

Table III-1. Summary of optical and electrochemical properties data of P-IsoPh-Br-T Salt and P-IsoPh-OH-T.

Polymer	UV-vis absorption spectra		Photoluminescence Spectra		Cyclic voltammetry		E_g^{opt}
	solution	film	solution	film	HOMO	LUMO	
	λmax/nm	λmax/nm	λmax/nm	λmax/nm	(eV)	(eV)	(eV)
P-IsoPh-Br-T	279	317	-	-	6.23	3.46	2.45
P-IsoPh-Br-T Salt	280	292	500	564	-	-	2.55
P-IsoPh-OH-T	471	473	543	545	5.55	3.53	2.28

II-3-3. Interfacial Properties

In order to evaluate the interface interaction between P-IsoPh-Br-T salt and P-IsoPh-OH-T to the ITO or ZnO, Kelvin Probe Microscopy (KPM) was used to calculate the effective work function (WF). It has been reported that presence of ZnO could reduce the ITO WF.[68] The WFs of bare ITO, ITO/P-IsoPh-Br-T salt and ITO/P-IsoPh-OH-T were -4.8, -4.44, and -4.46 eV, respectively. It was also observed that the WF of ITO/ZnO, ITO/ZnO/ P-IsoPh-Br-T salt and ITO/ZnO/ P-IsoPh-OH-T were -4.45, -4.2, -3.87 eV respectively (Figure III-5). Thus, the WF decreased after being modified by P-IsoPh-Br-T salt and P-IsoPh-OH-T indicates the formation of a favorable interface dipole which can lower the Schottky barrier and facilitate charge injection.[64]

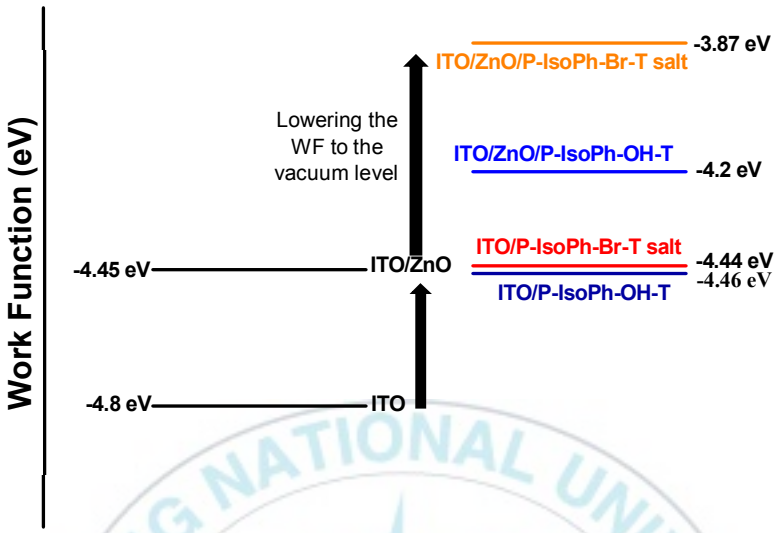

Figure III-5. Work function data from a matrix of the ITO electrodes coated with P-IsoPh-Br-T salt, P-IsoPh-OH-T and ZnO/P-IsoPh-Br-T salt, ZnO/P-IsoPh-OH-T salt film.

III-3-4. Photovoltaic properties

To investigate the cathode modification properties of P-IsoPh-Br-T salt in OSC, BHJ PSCs with device structure ITO / ZnO / CIL / PTB7:$PC_{71}BM$ / MoO_3 / Ag were fabricated. The alcohol soluble polymer with four terminal hydroxyl group, P-IsoPh-OH-T, also being invented and fabricated to IPSCs. The ZnO/MeOH device was a role as a reference. The current density-voltage (J-V) curves of the PSCs were measured under AM 1.5G irradiation (100 mW cm^{-2}) and are shown in Figure III-4. The corresponding photovoltaic parameters including V_{oc}, J_{sc}, FF, and PCE estimated from J-V curves are summarized in Table III-2.

The device achieved the best PCE of 7.52% for **P-IsoPh-Br-T salt** (with J_{sc}= 14.63 mA cm^{-2}, V_{oc}= 0.73 V, and FF= 70.5%), and 7.22 % for **P-IsoPh-OH-T** (with J_{sc}= 13.91 mA cm^{-2}, V_{oc}= 0.74 V, and FF= 70.2%), respectively. The polymer without electrolytes, **P-IsoPh-OH-T,** exhibit similar performance with the reference. The polymer with four quaterammonium salts in each monomer, **P-IsoPh-Br-T salt**, succeeded surpassing the PCE of the MeOH-treated ZnO by enhancing 0.3%. The main reason of the higher PCEs of **P-IsoPh-Br-T salt**, possibly due to the formation of a net

dipolar at the electrode interface of electrolytes modified **P-IsoPh-Br-T**, which is beneficial for the charge extraction and the suppression of recombination at the interface.[69]

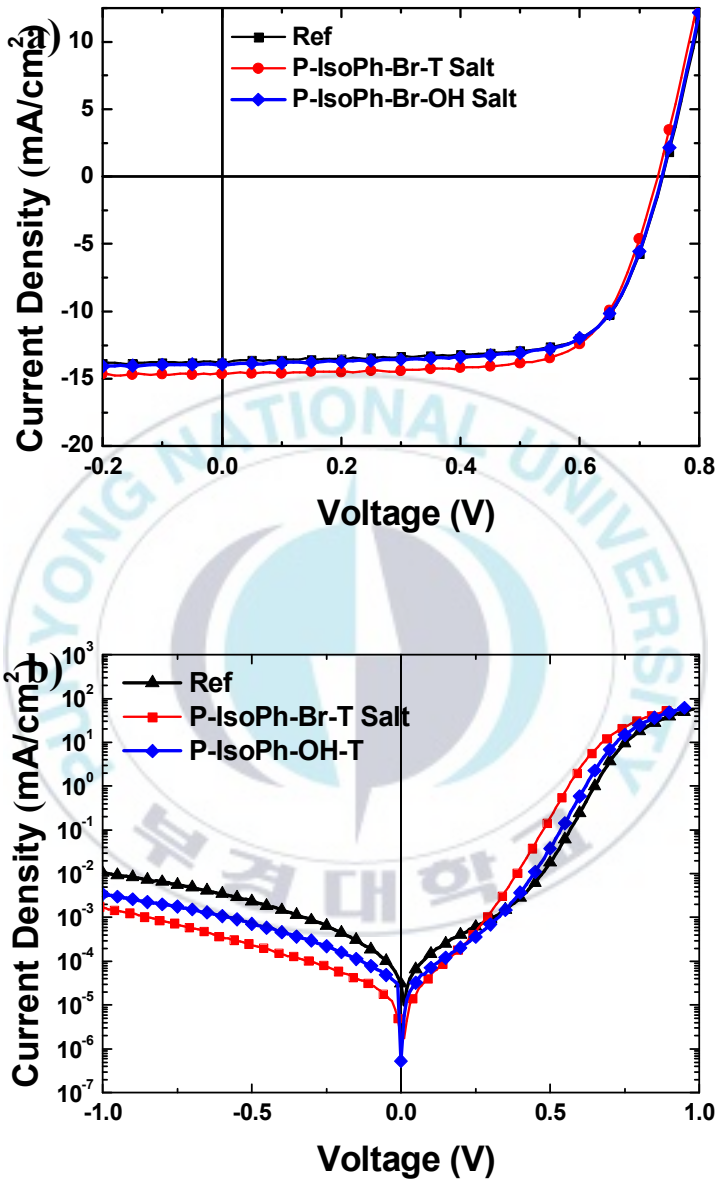

Figure III-6. Current density–voltage curves of P-IsoPh based CILs under AM 1.5G simulated illumination with an intensity of 100 mW/cm^2 (a) and under the dark condition (b).

Table III-2. Photovoltaic properties of inverted devices using P-IsoPh based CILs under AM 1.5G irradiation (100 mW cm^{-2}).

Sample Name	Jsc (mA/cm^2)	Voc (V)	FF (%)	PCE (%)
ZnO/MeOH	-14.65(-14.25)	0.76(0.75)	66.6(66.2)	7.41(7.08)
ZnO/ P-IsoPh-Br-T salt	14.63 (14.49)	0.73 (0.73)	70.5 (70.20)	7.52 (7.47)
ZnO/ P-IsoPh-OH-T	13.91 (13.69)	0.74 (0.74)	70.2 (70.45)	7.22 (7.09)

The averages for the photovoltaic parameters of each device are given in parentheses.

III-4. Conclusion

We have synthesized and characterized the alcohol soluble conjugated polymer **P-IsoPh-Br-T salt** and **P-IsoPh-OH-T** containing pendant amino groups and a carboxyl group, respectively as cathode interfacial materials for polymer solar cells. The XPS result clearly reports that P-IsoPh-Br-T succeeded convert to **P-IsoPh-Br-T salt**. The two polymers are promising as a hole blocking layer with deep HOMO levels. The **P-IsoPh-Br-T salt and P-IsoPh-OH-T** demonstrates a strong impact on the interfacial interaction to the electrode by reducing the work function of ITO. As a result, this polymer work efficiently and achieved a PCE of 7.52% for **P-IsoPh-Br-T salt** based device. The result indicated that formation of a net dipolar at the electrode interface by **P-IsoPh-Br-T salt**, leading to better enhanced the device performance of the solar cell.

Chapter IV. Conjugated oligo-electrolytes as cathode interfacial layer for IPSCs

IV-1. Introduction

The charge injecting/collecting properties are related to the interfacial properties between the semiconducting layer and the cathode or the anode. Conjugated oligomers electrolytes, alcohol-soluble conjugated polymers have been mainly applied to the solution processable cathode interface layer of organic electronic devices. In this chapter, new small molecule type of interfacial layer material based on fluorene derivative for the applications in organic solar cells will be introduced.

IV-2. Experimental

IV-2-1. Material and synthesis

IV-2-1-1. Materials

Toluene was bubbling with nitrogen. All other chemicals were purchased from Sigma-Aldrich co, Alfa Aesar (A Johnson Matthey

Company) or Toyo Chemical Industry (TCI) and were used as received unless otherwise described.

IV-2-1-2. Synthesis

IV-2-1-2-1. General procedure of Suzuki coupling reaction

A mixture of aryl bromide, aryl boronic ester, 5.0 mol % of tetrakis(triphenylphosphine) palladium [$Pd(PPh_3)_4$] and several drops of aliquat336 in degassed 1:1 (by volume) mixed solvent of Toluene and 2M K_2CO_3 aqueous was stirred for 12-18 hours at 80 ºC under the N_2 atmosphere. A portion of 100 mL of water has added the mixture and allowed to cool to room temperature. The mixture was extracted with MC and the extracted organic layer was dried over anhydrous $MgSO_4$. The organic solvent was removed by using a rotary evaporator.

IV-2-1-2-2. General procedure of stille coupling reaction

A mixture of aryl bromide, tin compound, and 5.0 mol % of bis(diphenyl-phosphino)ferrocene] palladium (II) dichloride [$Pd(dppf)Cl_2$] in toluene was stirred for 6-18 hours at 110 ºC under N_2 atmosphere. A portion of 100 mL of water has

added the mixture and allowed to cool to room temperature. The mixture was extracted with MC and the extracted organic layer was dried over anhydrous $MgSO_4$. The organic solvent was removed by using a rotary evaporator.

IV-2-1-2-3. Synthesis of 2-bromo-9,9-bis-(6-bromo-hexyl)-9H-fluorene (2)

A mixture of compound (1) 2-Bromo-9H-fluorene (4.9 g, 20.00 mmol), 1,6-Dibromo-hexane (97.6 ml, 400.00 mmol), 30 mL of 2M KOH solution in water and 5.0 mol % of PTC (0.693 g, 0.100 mmol) was stirred for 18 hours at 80 ^oC under N_2 atmosphere. A portion of 100 mL of water has added the mixture and allowed to cool to room temperature. The mixture was extracted with Methylene chloride (MC) and the extracted organic layer was dried over anhydrous $MgSO_4$. The organic solvent was removed by using a rotary evaporator. The excess of 1,6-Dibromo-hexane was recovered by vacuum distillation. The crude product was purified by column chromatography on silica gel using MC/n-hexane. The yield of light yellow liquid was 3.220 g (56.3%). ^{1}H-NMR (400 MHz, $CDCl_3$, ppm): δ 7.69~7.66 (m, 1H), 7.57~7.55 (dd, J_1=1.5

Hz, J_2=1.5 Hz, 1H), 7.47~7.45 (dd, J_1=1.9 Hz, J_2=1.4 Hz, 2H), 7.36~7.30 (m, 3H), 3.30~3.27 (t, J=6.95, 4H), 2.01~1.88 (m, 4H), 1.69~1.62 (m, 4H), 1.23~1.03 (m, 4H), 1.11~1.03 (m, 4H), 0.65~0.54 (m, 4H). ^{13}C-NMR (400 MH z, $CDCl_3$, ppm): δ 150.05, 147.83, 141.03, 133.55, 130.62, 129.66, 126.67, 122.55, 123.22, 121.61, 52.16, 43.91, 34.04, 32.57, 29.39, 28.10, 24.37.

IV-2-1-2-4. Synthesis of 4,4,5,5,4',4',5',5'-Octamethyl-[2,2']bi[[1,3,2]dioxa-borolanyl]-Benzene (4)

To a round bottom (RB) flask two-neck was charged a mixture of compound (3) 1,4-dibromo-benzene (5 g, 21.19 mmol), bis(pinacolato)diboron (32.29 gr, 127.08 mmol), potassium acetate (8.31 gr, 84.77 mmol) and [Pd(dppf)Cl_2] as a catalyst. The RB flask was pumped under vacuum and refilled with nitrogen. To the mixture was charged *N,N*-dimethylformamide (10 mL, charged via syringe). The resulting mixture was heated to 100 ^{o}C and stirred at this temperature under nitrogen for 18 h, and then cooled to room temperature. To the mixture was added water (50 mL) and ethyl acetate (50 mL). The ethyl acetate layer was separated, washed with water (50 mL x 2) and brine, dried over magnesium sulfate,

concentrated, and purified by flash column chromatography (hexanes and ethyl acetate as eluents) to provide the desired benzene boronic ester. ^{1}H-NMR (400 MHz, $CDCl_3$, ppm): δ 7.80 (s, 1H), 1.35 (s, 6H). ^{13}C-NMR (400 MHz, $CDCl_3$, ppm): δ 133.40, 131.52, 88.13, 24.77.

IV-2-1-2-5. Synthesis of 2,5-bis-[9,9-bis-(6-bromo-hexyl)-9H-fluoren-2-yl]-Benzene (FBF)

This trimmer FBF was synthesized by Suzuki coupling reaction. The benzene boronic ester (4) (0.33 gr, 1 mmol), the 2-bromo-9,9-bis-(6-bromo-hexyl)-9H-fluorene(2) (1.43 gr, 2.5 mmol), 5% mol of tetrakis(triphenylphosphine) palladium [Pd(PPh3)4] (0.058 g, 0.050 mmol), and several drops of aliquat. 336 in 20 mL of degassed 1:1 (by volume) mixed solvent of toluene and 2M K_2CO_3 aqueous was stirred for 72 hours at 110 ºC under the N_2. A portion of 100 mL of water has added the mixture and allowed to cool to room temperature. The mixture was extracted with methylene chloride (MC) and the extracted organic layer was dried over anhydrous $MgSO_4$. The organic solvent was removed by using a rotary evaporator. The crude product was purified by column

chromatography on silica gel using MC/n-hexane. The yield of yellow sticky liquid was 0.72 g (68%). ^{1}H-NMR (400 MHz, $CDCl_3$, ppm): δ 7.80~7.79 (d, *J*=5 Hz, 3H), 7.76~7.74 (d, *J*=7.3 Hz, 1H), 7.67~7.65 (d, *J*=7.7 Hz, 1H), 7.60 (s, 1H), 7.41~7.33 (m, 3H), 3.30~3.27 (t, *J*=6.8, 4H), 2.0542~2.0130 (m, 4H), 1.6998~1.6284 (m, 4H), 1.2327~1.1750 (m, 4H), 1.13~1.06 (m,4H), 0.71~0.66 (m,4H). ^{13}C-NMR (400 MHz, $CDCl_3$, ppm): δ 151.85, 151.38, 141.47, 140.36, 128.32, 127.94, 123.57, 122.04, 120.84, 120.60, 55.80, 41.03, 34.73, 33.39, 29.82, 28.51, 24.33.

IV-2-1-2-6. Synthesis of 2,5-bis-[9,9-bis-(6-bromo-hexyl)-9H-fluoren-2-yl]-thiophene (FTF)

This trimmer FTF was synthesized by stille coupling reaction. The 2,5-bis-tributylstannanyl-thiophene (0.4 mmol) and the 2-bromo-9,9-bis-(6-bromo-hexyl)-9H-fluorene(2) (1 mmol) were mixed in degassed toluene. [Pd(dppf)Cl_2] (22 mg) were added to the mixture as a catalyst. The reaction mixture was stirred and heated to reflux for 48 h under N_2 atmosphere. A portion of 100 mL of water has added the mixture and allowed to cool to room temperature. The mixture was extracted with methylene chloride (MC) and the

extracted organic layer was dried over anhydrous $MgSO_4$. The organic solvent was removed by using a rotary evaporator. The crude product was purified by recrystallization using methanol. The yield of red powder was 0.37 g (85%). ^{1}H-NMR (400 MHz, $CDCl_3$, ppm): δ 7.72~7.70 (t, J=3.8 Hz, 2H), 7.63~7. 60 (m, 1H), 7.55 (s, 1H), 7.38~7.32 (m, 4H), 3.30~3.27 (t, J=6.75 Hz, 4H), 2.05~1.99 (m, 4H), 1.70~1.62 (m, 4H), 1.22~1.17 (m, 4H), 1.13~1.06 (m,4H), 0.66~0.63 (m,4H). ^{13}C-NMR (151 MHz, $CDCl_3$, ppm): δ 151.25, 149.82, 141.47, 139.87, 133.98, 128.01, 127.84, 125.39, 121.10, 120.41, 55.82, 51.66, 41.01, 34.74, 33.37, 29.79, 28.50, 24.27.

IV-2-1-2-7. Synthesis of 6,6',6'',6'''-(phenyl-2,5-diylbis(9H-fluorene-9,9,2-triyl))tetrakis(N,N,N-trimethylhexan-1-aminium) bromide (FBF Salt)

The Trimer FBF was synthesized by Suzuki coupling reaction as mentioned before. Then, the ionic FBF salt was obtained by treating 2,5-bis-[9,9-bis-(6-bromo-hexyl)-9H-fluoren-2-yl]-Benzene with trimethylamine in THF for 6 days, followed by extraction with water. The water was then removed under reduced

pressure. The trimer was dried in vacuum overnight and was obtained as a yellow solid. ^{1}H NMR (600 MHz, METHANOL-D3) δ 7.88~7.84 (m, 2H), 7.81~7.78 (d, J = 7.6 Hz, 1H), 7.79~7.75 (m, 2H), 7.72~7.66 (m, 2H), 7.48~7.40 (m, 1H), 3.24~3.16 (m, 4H), 3.02 (s, 18H), 2.23~2.03 (m, 4H), 1.61~1.46 (m, 4H), 1.19~1.08 (m, 8H), 0.72~0.56 (m, 4H).

IV-2-1-2-8. Synthesis of 6,6',6'',6'''-(thiophene-2,5-diylbis(9H-fluorene-9,9,2-triyl))tetrakis(N,N,N-trimethylhexan-1-aminium) bromide (FTF Salt)

The Trimer FTF was synthesized by stille coupling reaction as mentioned before. Then, the ionic FTF salt was obtained by treating 2,5-bis-[9,9-bis-(6-bromo-hexyl)-9H-fluoren-2-yl]-thiophene with trimethylamine in THF for 6 days, then the solvent was removed. The trimer was dried in vacuum overnight and was obtained as a red solid. ^{1}H NMR (600 MHz, METHANOL-D3) δ 7.78~7.71 (m, 2H), 7.69~7.67 (m, 1H), 7.44~7.27 (m, 4H), 3.19~3.08 (m, 4H), 2.99 (s, 18H), 2.16~1.98 (m, 4H), 1.47~1.42 (m, 4H), 1.18~1.02 (m, 8H), 0.59~0.52 (m, 4H).

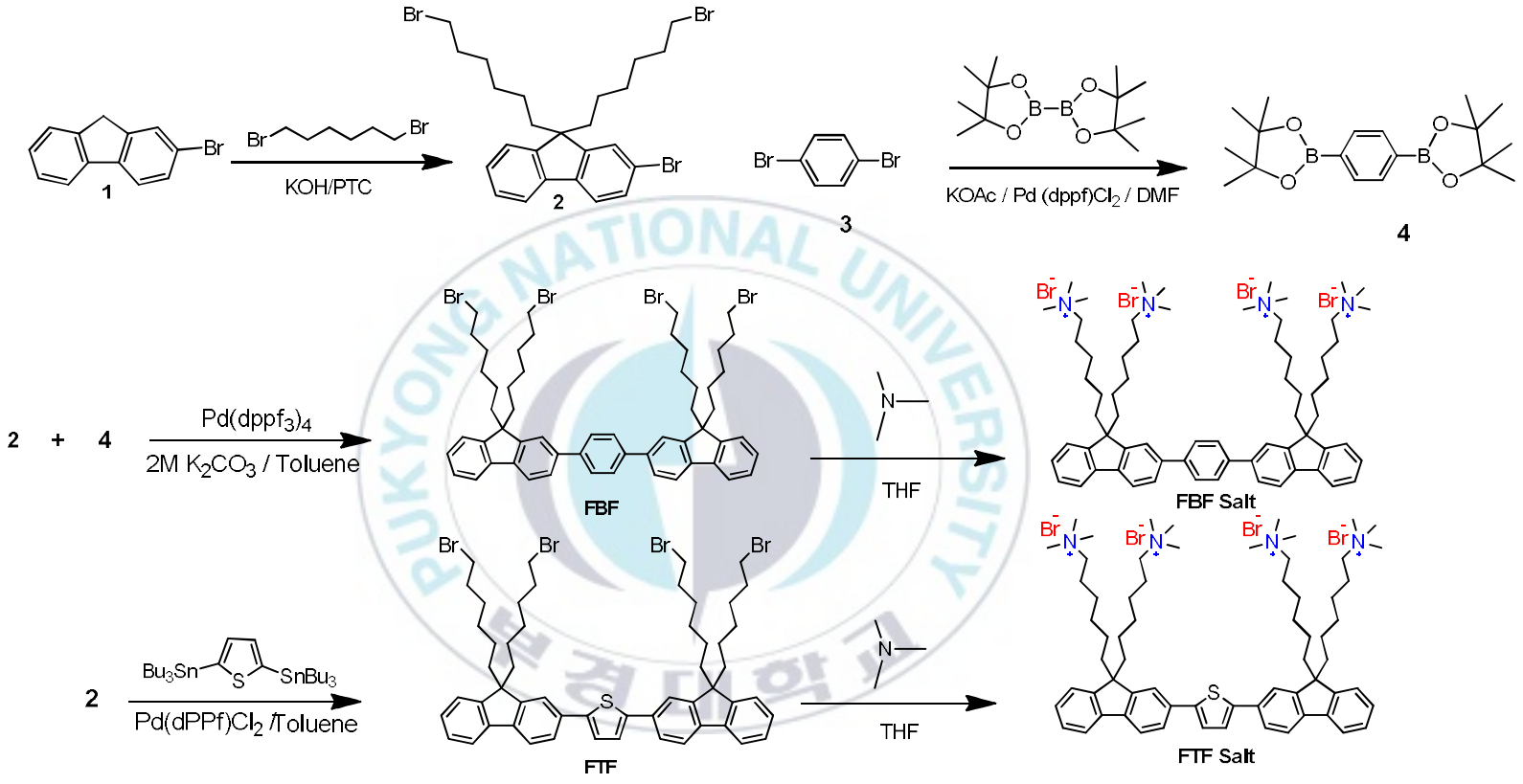

Scheme IV-1. Synthesis of conjugated Trimer I

IV-2-1-2-9. Synthesis of 2,2'-(9,9-bis(6-bromohexyl)-9H-fluorene-2,7-diyl) dithiophene (TFT)

This trimmer TFT was synthesized by Suzuki coupling reaction. The 4,4,5,5-tetramethyl-2-(thiophen-2-yl)-1,3,2-dioxaborolane (6 mmol) and the 2-bromo-9,9-bis-(6-bromo-hexyl)-9H-fluorene (2) (2 mmol) were mixed in degassed Toluene. $[Pd(pph)_3]_4$ (10%mol. 0.2 mmol, 0.23 gr) were added to the mixture as catalyst. The reaction mixture was stirred and heated to 110℃. A few drops of tetraethylammonium (TEA) was added to the mixture after the reflux temperature reached. The reaction time was 72 h under N_2 atmosphere. A portion of 100 mL of water was added the mixture and allowed to cool to room temperature. The mixture was extracted with methylene chloride (MC) and the extracted organic layer was dried over anhydrous $MgSO_4$. The organic solvent was removed by using a rotary evaporator. The crude product was purified by column chromatography on silica gel using MC/n-hexane. The yield of red powder was 0.42 g (54%). MS: $[M^+]$, m/z 656. ^{1}H-NMR (400 MHz, $CDCl_3$, ppm): δ 7.69~7.67 (d, J=10.1 Hz, 2H), 7.62~7.60 (dd, J=7.9 Hz, 2H), 7.55~7.54 (d, J=1.5 Hz, 2H), 7.39~7.38 (dd, J=3.6 Hz, 2H), 7.32~7.29 (m, 2H), 7.12~7.10

(m, 2H), 3.27~3.24 (t, *J*=11.5 Hz, 4H), 2.04~1.99 (m, 4H), 1.67~1.60 (m, 4H), 1.21~1.15 (m, 4H), 1.12~1.05 (m, 4H), 0.71~0.63 (m, 4H). ^{13}C-NMR (151 MHz, $CDCl_3$, ppm): δ 152.07, 145.74, 140.95, 134.14, 128.87, 125.86, 125.39, 123.74, 120.94, 120.78, 55.92, 51.66, 41.02, 34.70, 33.36, 29.76, 28.49, 24.28.

IV-2-1-2-10. Synthesis of 9,9-bis (6-bromohexyl)- 2,7-diphenyl-9H-fluorene (BFB)

This trimer BFB was synthesized by Suzuki coupling reaction. The phenylboronic acid (0.366 gr, 3 mmol), the 2-Bromo-9,9-bis-(6-bromo-hexyl)-9H-fluorene(2) (0.65 gr, 1 mmol), 10% mol of tetrakis(triphenylphospine) palladium [$Pd(PPh_3)_4$] (0.1 mmol, 0.115 gr), and several drops of aliquat. 336 in 20 mL of degassed 1:1 (by volume) mixed solvent of toluene and 2M K_2CO_3 aqueous was stirred for 72 hours at 110 ^oC under the N_2. A portion of 100 mL of water was added the mixture and allowed to cool to room temperature. The mixture was extracted with methylene chloride (MC) and the extracted organic layer was dried over anhydrous $MgSO_4$. The organic solvent was removed by using a rotary evaporator. The crude product was purified by column

chromatography on silica gel using MC/n-hexane. The yield of red powder was 0.44 g (68%). MS: [M^+], m/z 644. ^{1}H NMR (600 MHz, $CDCl_3$, ppm) δ 7.82~7.77 (t, J = 8.2 Hz, 1H), 7.74~7.68 (dd, J = 11.4, 4.0 Hz, 2H), 7.65~7.61 (t, J = 7.5 Hz, 1H), 7.60~7.57 (d, J = 7.3 Hz, 1H), 7.54~7.47 (m, 2H), 7.42~7.36 (dd, J = 14.8, 7.4 Hz, 1H), 3.33~3.23 (m, 2H), 2.12~1.99 (d, J = 7.6 Hz, 2H), 1.72~1.60 (m, 2H), 1.25~1.19 (dd, J = 14.1, 6.5 Hz, 2H), 1.15~1.04 (m, 2H), 0.79~0.67 (m, 2H). ^{13}C NMR (151 MHz, $CDCl_3$, ppm) δ 151.37, 141.63, 140.33, 128.91, 127.45, 126.30, 121.51, 120.21, 55.25, 40.43, 34.08, 32.74, 29.82, 29.18, 27.87, 23.70.

IV-2-1-2-11. Synthesis of 9,9-bis(6-bromohexyl)-2,7-bis(2,4-difluoro-phenyl)- 9H-fluorene (BfFBf)

This trimmer BfFBf was synthesized by Suzuki coupling reaction. The (2,4-difluorophenyl)boronic acid (6 mmol) and the 2-bromo-9,9-bis-(6-bromo-hexyl)-9H-fluorene (2) (1.3 gr, 2 mmol) were mixed in degassed toluene. $[Pd(pph)_3]_4$ (10%mol. 0.2 mmol, 0.23 gr) were added to the mixture as a catalyst. The reaction mixture was stirred and heated to 110℃. A few drops of tetraethylammonium (TEA) was added to the mixture after the

reflux temperature reached. The reaction time was 72 h under N_2 atmosphere. A portion of 100 mL of water has added the mixture and allowed to cool to room temperature. The mixture was extracted with methylene chloride (MC) and the extracted organic layer was dried over anhydrous $MgSO_4$. The organic solvent was removed by using a rotary evaporator. The crude product was purified by column chromatography on silica gel using MC/n-hexane. The yield of red powder was 0.98 g (67%). MS: [M^+], m/z 716. ^{1}H-NMR (400 MHz, $CDCl_3$, ppm): δ 7.80~7.78 (d, J=7.7 Hz, 2H), 7.52~7.46 (m, 6H), 7.0172~6.9183 (m, 4H), 3.2870~3.2522 (t, J=6.95 Hz, 4H), 2.0414~2.002 (m, 4H), 1.69~1.62 (m, 4H), 1.26~1.18 (m, 4H), 1.13~1.06 (m, 4H), 0.77~0.69 (m, 4H). ^{13}C-NMR (151 MHz, $CDCl_3$, ppm): δ 161.87, 159.38, 151.70, 140.98, 134.70, 132.28, 128.65, 124.19, 112.43, 105.21, 55.94, 40.90, 33.52, 32.71, 29.75, 28.45, 24.33.

IV-2-1-2-12. Synthesis of 6,6'-(2,7-di(thiophen-2-yl)-9H-fluorene-9,9-diyl) bis(N,N,N-trimethylhexan-1-aminium) bromide (TFT Salt)

The Trimer TFT was synthesized by Suzuki coupling reaction as mentioned before. Then, the ionic TFT salt was obtained by treating 2,2'-(9,9-bis(6-bromohexyl)-9H-fluorene-2,7-diyl) dithiophene with trimethylamine in THF for 6 days, then the solvent was removed. The trimer was dried in vacuum overnight and was obtained as a light yellow powder. 1H NMR (600 MHz, METHANOL-D3) δ 7.74 – 7.72 (m, 1H), 7.69 – 7.67 (d, J = 1.2 Hz, 1H), 7.65 – 7.61 (dd, J = 7.9, 1.5 Hz, 1H), 7.51 – 7.48 (dd, J = 3.4, 0.6 Hz, 1H), 7.39 – 7.37 (m, 1H), 7.12 – 7.10 (t, J = 5.1, 2.5 Hz, 1H), 3.14 – 3.09 (m, 2H), 2.93 (s, 9H), 2.14 – 2.09 (m, 2H), 1.49 – 1.42 (m, 2H), 1.11 – 1.05 (m, 4H), 0.66 – 0.59 (m, 2H).

IV-2-1-2-13. Synthesis of 6,6'-(2,7-diphenyl-9H-fluorene-9,9-diyl) bis(N,N,N-trimethylhexan-1-aminium) bromide (BFB Salt)

The Trimer BFB was synthesized by Suzuki coupling reaction as mentioned before. Then, the ionic BFB salt was obtained by

treating 9,9-bis (6-bromohexyl)- 2,7-diphenyl-9H-fluorene with trimethylamine in THF for 6 days, then the solvent was removed. The trimer was dried in vacuum overnight and was obtained as a white powder. 1H NMR (600 MHz, METHANOL-D3) δ 7.83 – 7.79 (m, 1H), 7.71 – 7.69 (m, 3H), 7.64 – 7.61 (m, 1H), 7.48 – 7.44 (m, 2H), 7.36 – 7.32 (m, 1H), 3.15 – 3.11 (m, 2H), 2.93 (s, 9H), 2.18 – 2.13 (m, 2H), 1.51 – 1.43 (m, 2H), 1.17 – 1.06 (m, 4H), 0.71 – 0.62 (m, 2H).

IV-2-1-2-14. Synthesis of 6,6'-(2,7-bis(2,4-difluorophenyl)-9H-fluorene-9,9-diyl)bis(N,N,N-trimethylhexan-1-aminium) bromide (BfFBf Salt)

The Trimer BfFBf was synthesized by Suzuki coupling reaction as mentioned before. Then, the ionic BfFBf salt was obtained by treating 9,9-bis(6-bromohexyl)-2,7-bis(2,4-difluoro-phenyl)- 9H-fluorene with trimethylamine in THF for 6 days, then the solvent was removed. The trimer was dried in vacuum overnight and was obtained as a white powder. 1H NMR (600 MHz, METHANOL-D3) δ 7.87~7.83 (d, J = 7.9 Hz, 1H), 7.61~7.56 (m, 2H), 7.52~7.49 (d, J = 7.8 Hz, 1H), 7.11~7.06 (m, 2H), 3.20~3.15 (dd, J = 10.1,

7.0 Hz, 2H), 3.01 (s, 9H), 2.14~2.08 (m, 2H), 1.56~1.51 (m, 2H), 1.17~1.11 (m, 4H), 0.71~0.64 (m, 2H).

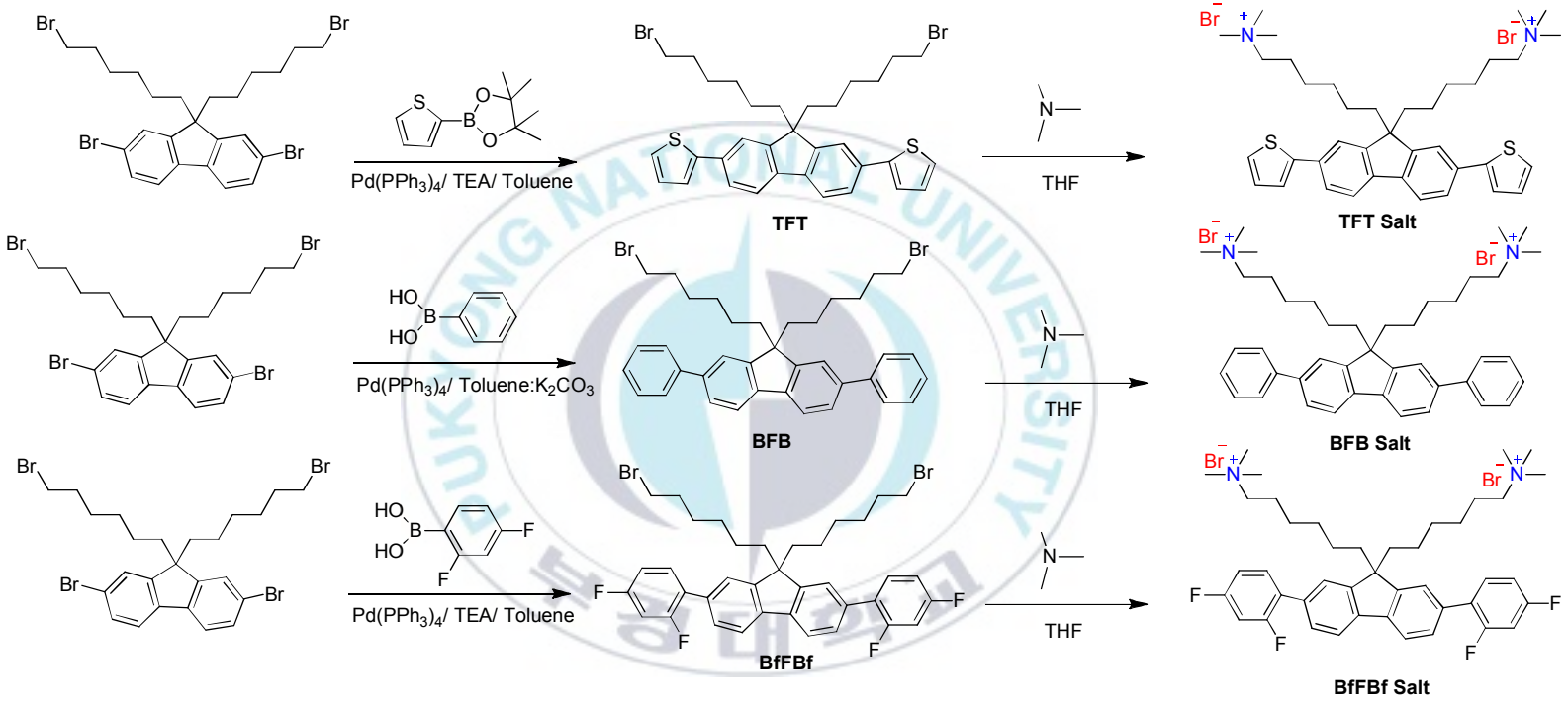

Scheme IV-2. Synthesis of conjugated Trimer II

IV-2-2. Fabrication of PSCs

In order to fabricate the inverted type organic photovoltaic (OPV) with the device structure: [ITO/ZnO (40 nm)/ ETL (~ 5 nm)/active layer (PTB7:$PC_{71}BM$, 100 nm)/MoO_3 (10 nm)/Ag (100 nm)], a ZnO layer was deposited on an ITO substrate by the sol-gel process. A thin film of ZnO sol-gel precursor was cured at 200 °C for 10 min. A thin layer of interlayer material was prepared by spin coating with a MeOH solution of oligomer compound (1 mg/mL) at 4000~5000 rpm for 60 seconds onto the ITO or ZnO. The typical thickness of a cathode buffer layer was less than 5 nm at room temperature. The active layer was spin-cast from a mixture of PTB7 and $PC_{71}BM$ (obtained by dissolving 10 mg of PTB7 and 15 mg of $PC_{71}BM$ in 1 mL of chlorobenzene with 3% (w/v) 1,8-diiodooctane (DIO)) and stirring at 2000 rpm for 120 s. The active solution was then filtered through a 0.2 m membrane filter δ before spin coating. Successive layers of MoO_3 and Ag were thermally evaporated through a shadow mask, with a device area 13 mm^2 at 2 x 10^{-6} Torr.

IV-2-3. Measurement

Synthesized compounds were characterized by ^{1}H and ^{13}C NMR spectra, and it was recorded on a JEOL JNM ECP-400 spectrometer. The elemental MASS analysis of synthesized compounds was carried out on an Elementar Vario macro/micro elemental analyzer, Shimadzu GC-MS QP-5050A spectrometer and Perkin-Elmer Voyager- DE PRO. UV-Visible spectra were recorded using UV-Vis spectrophotometer (JASCO V-530). Cyclic voltammetry (CV) was performed by an Ivium B14406 with a three-electrode cell in a solution of 0.10 M tetrabutylammonium hexafluorophosphate (Bu_4NPF_6) in acetonitrile anhydrous at a scan rate of 100 mV/s. Pt coil and wire were used as the counter and working electrode, respectively. An Ag/Ag^{+} electrode was used as the reference electrode. Prior to each measurement, the cell was deoxygenated with nitrogen. Elemental analysis was performed using X-ray photoelectron spectroscopy (XPS) (Thermo VG Scientific (UK), MultiLab2000) and recorded using Al Kα X-ray line (15 kV, 300 W). Kelvin probe microscopy (KPM) measurements (KP Technology Ltd. Model KP020) were performed on the ZnO layers, with and without ETL, and the work

function of the samples were estimated by measuring the contact potential difference between the sample and the KPM tip. The KPM tip was calibrated against a standard reference gold surface, with a work function of 5.1 eV. The current density–voltage measurements were performed under simulated light (AM 1.5G, 1.0 sun condition/100 mW/cm^2) from a 150 W Xe lamp, using a KEITHLEY Model 2400 source measure unit. A calibrated Si reference cell with a KG5 filter certified by National Institute of Advanced Industrial Science and Technology was used to confirm 1.0 sun condition.

IV-3. Result and Discussion

IV-3-1. XPS elemental analysis

The chemical structure of all oligomer salt was confirmed by X-ray photoelectron spectroscopy (XPS) in figure IV-1. All oligo-electrolytes exhibits new N 1s peak around ~400 eV and all oligomers before quaternization reaction did not have N 1s peaks. We conclude that the reaction to convert all oligomer become oligo-electrolytes was succeeded.

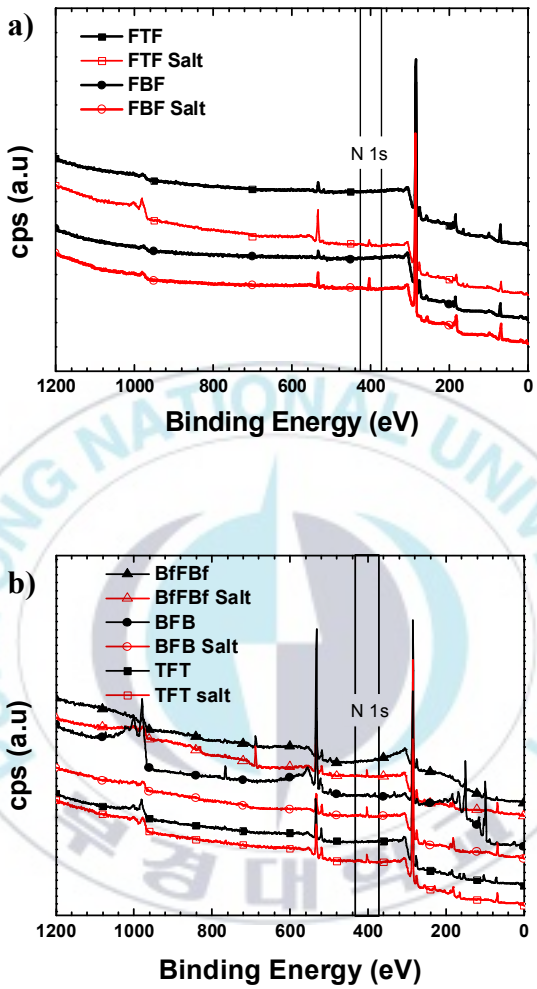

Figure IV-1. Survey X-ray photoelectron spectra (a) FTF, FBF, (b) TFT, BfFBf, and BFB with their quaternary ammonium salt.

IV-3-2. Optical and electrochemical properties

All of the oligomer electrolytes are alcohol soluble and it has poor solubility in chlorobenzene and dichlorobenzene which is very important for inverted fabrication device. The absorption spectra and cyclic voltammogram (CV) of all oligomers are provided in Figure IV-2 and figure IV-3. The UV-Vis of all oligomers obtained in chloroform solution and all oligo-electrolytes obtained in methanol solution. From the CV we can calculate the HOMO and LUMO of the materials using the onset point in oxidation process and reduction process, respectively. The optical bandgap could be obtained from absorption edge of the oligomers. The corresponding absorption peaks, energy level data and optical bandgap are summarized in Table IV-1.

FTF salt and **FBF salt** showed an absorption maximum (λ_{sbs}) at 381 and 330 nm in solution state while **TFT salt**, **BFB salt** and **BfFBf salt** showed an absorption band peaks at 351, 327, and 317 nm, respectively. In the case of all oligomers thin film, λ_{sbs} appeared red shifted and much broader at 392, 340, 360, 332, and 322 nm for **FTF salt**, **FBF salt, TFT salt**, **BFB salt** and **BfFBf salt**, respectively. The optical bandgaps (E_g) of **FTF salt** and **FBF**

salt were slightly lower than that of **TFT salt** and **BFB salt** due to their longer conjugation length. All oligo-electrolytes were similar in optical bandgap to analogous oligomers before quaternarization, indicating that ionic side chains did not influence their optical properties.[70, 71]

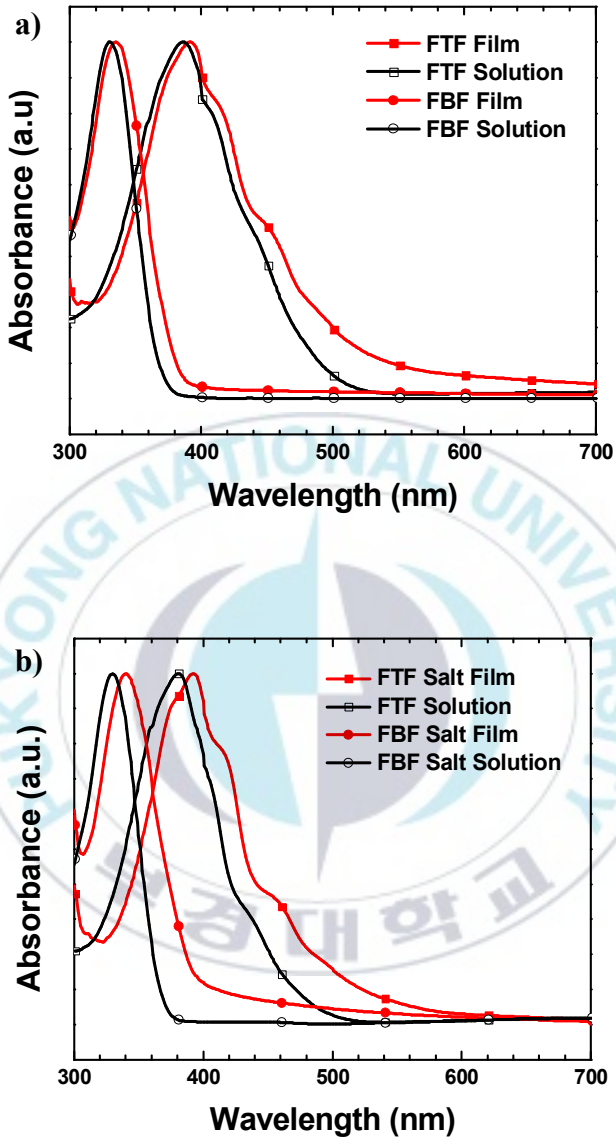

Figure IV-2. UV-Visible spectra of FTF and FBF in chloroform solution and thin film (a); and their quaternary ammonium salt, FTF salt and FBF salt in methanol solution and thin film (b).

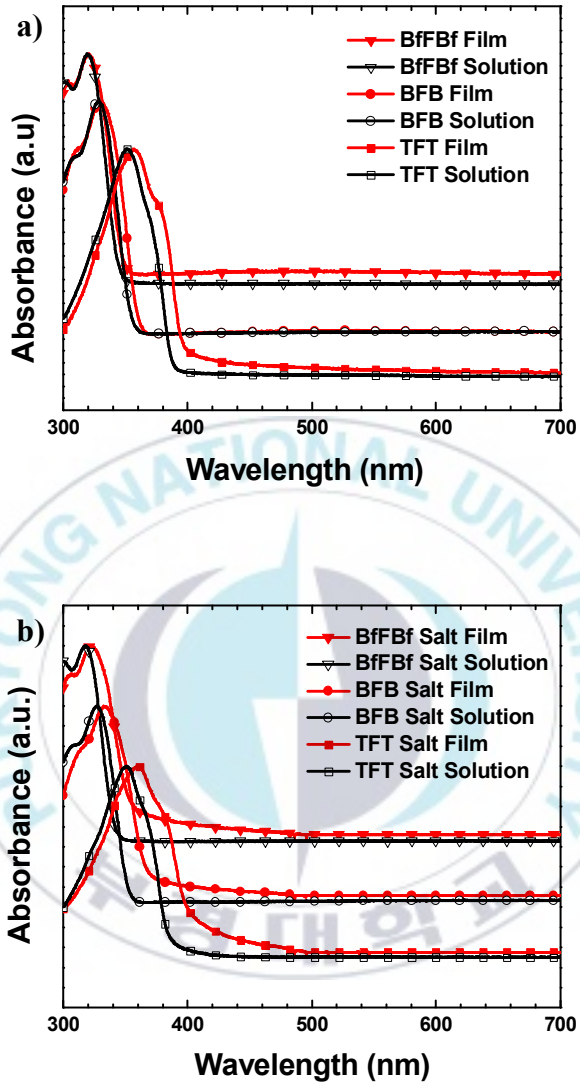

Figure IV-3. UV-Visible spectra of BfFBf, BFB and TFT in chloroform solution and thin film (a); and their quaternary ammonium salt, BfFBf salt, BFB salt and TFT salt in methanol solution and thin film (b).

The HOMO levels of for the oligomers were obtained from the onsets of the oxidation potential (E_{ox}) when cyclic voltammetry was performed in 0.1 mol/L of Bu_3NClO_4 in an acetonitrile solution (Figure IV-3). The HOMO values of **FTF**, **FBF, TFT**, **BFB** and **BfFBf** were thus calculated to be 5.54, 5.77, 5.27, 5.28 and 5.56 eV, respectively, using the ferrocene value of 4.8 eV below the vacuum as the internal standard.[62] The lowest unoccupied molecular orbital (LUMO) energy levels of the oligomers were estimated to be 3.29, 3.19, 3.27, 3.30 and 3.57 eV for **FTF**, **FBF, TFT**, **BFB** and **BfFBf**, respectively. In principle, the low-lying HOMO energy level of the conjugated main chains would be beneficial for hole blocking ability with respect to various donor materials in the photovoltaic devices.[67]

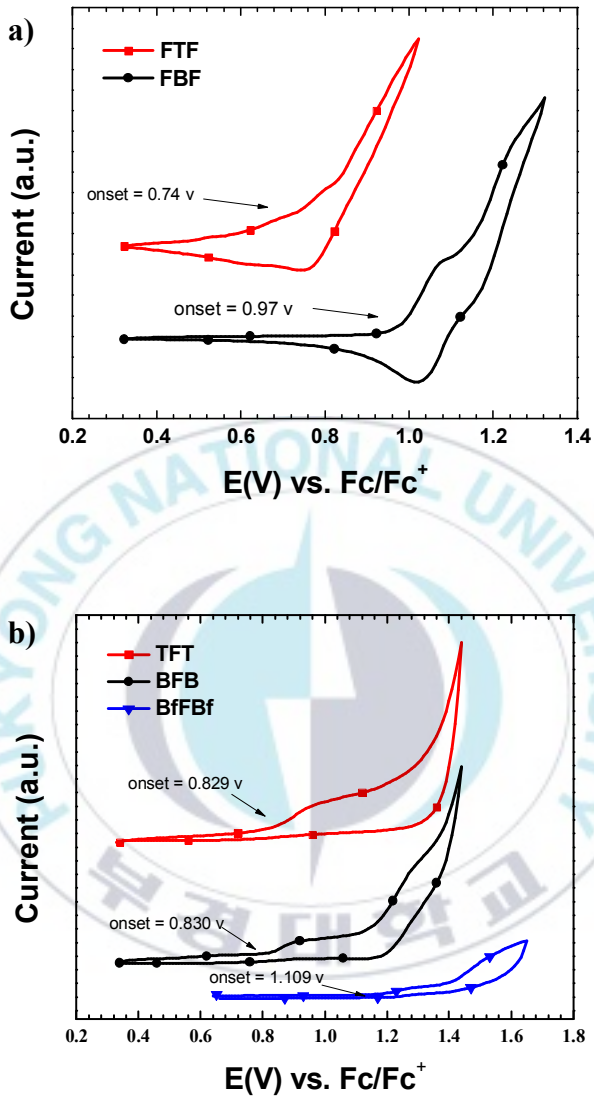

Figure IV-4. Cyclic Voltammogram of (a) FTF, FBF, (b) TFT, BFB, and BfFBF as films measured in 0.1 M Bu_4NPF_6 in acetonitrile

Table IV-1. Summary of optical and electrochemical properties data.

Interlayer	UV-vis absorption spectra		E_g^{opt}	Interlayer	UV-vis absorption spectra		E_g^{opt}	Cyclic voltammetry	
	Solution	Film			Solution	Film		HOMO	LUMO
	λmax/nm	λmax/nm	(eV)		λmax/nm	λmax/nm	(eV)	(eV)	(eV)
FTF Salt	381	392	2.35	FTF	386	392	2.25	5.54	3.29
FBF Salt	330	340	3.22	FBF	331	335	3.22	5.77	2.59
TFT Salt	351	360	3.18	TFT	351	355	3.20	5.27	3.27
BFB Salt	327	332	3.47	BFB	328	330	3.48	5.28	3.30
BfFBf Salt	317	322	3.49	BfFBf	318	320	3.50	5.56	3.57

IV-3-3. Interfacial properties

In order to evaluate the interface interaction between oligomers salts and ITO or ZnO, Kelvin Probe Microscopy (KPM) was used to calculate the effective work function (WF). As shown in the Figure IV-5, the WF of bare ITO down-shifted toward vacuum level to -4.16 eV for FTF salt, -4.02 for FBF salt, -4.53 for TFT salt, -4.47 for BFB salt and -4.55 for BfFBf salt, respectively. It has been reported that ZnO could decrease the WF of ITO.[68] Interestingly, FTF salt and FBF salt have a better result to reducing the work function of ITO than ZnO (the WF ITO/ZnO=-4.4 eV) indicating that FTF salt and FBF salt can provide a stronger interfacial interaction than ZnO does. In the other case, the FTF salt, FBF salt, TFT salt, BFB salt, and BfFBf salt could also lower the WF of ITO/ZnO by -4.14, -4.15, -3.94, -4.02, -4.15 eV, respectively. However, the WF decreased after being modified by oligomer salts indicates the formation of a favorable interface dipole which can lower the Schottky barrier and facilitate charge injection.[64]

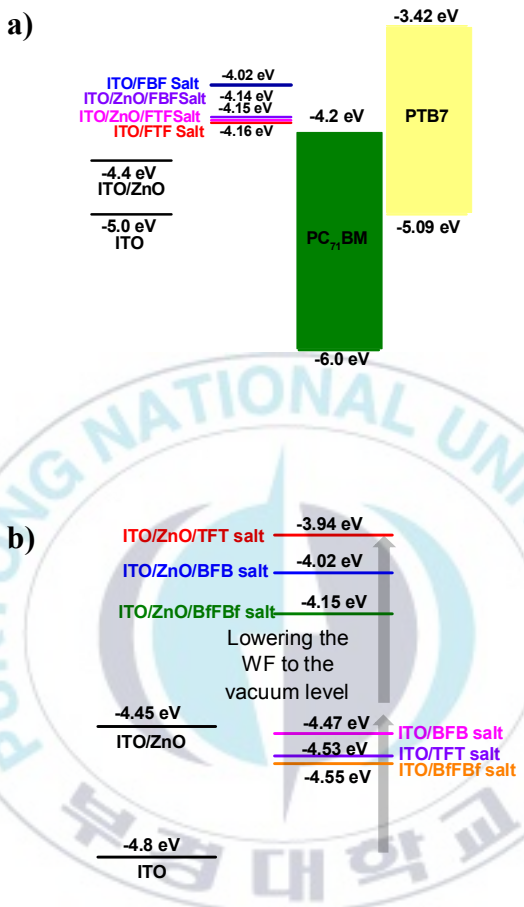

Figure IV-5. (a) Energy level diagram of PTB7:$PC_{71}BM$ and the improvement of ITO electrode by ZnO, FTF salt and FBF salt; (b) Work function data from a matrix of the ITO electrodes coated with TFT salt, BFB salt, BfFBf salt and the ZnO film.

IV-3-4. Photovoltaic properties

Inverted polymer solar cells (I-PSCs) were fabricated with the configuration of ITO/ZnO/CIL/active layer/MoO_3/Ag to study the interfacial function of all oligomer salts. In this inverted device structure, ITO was used as the cathode, Ag was used as the anode, and PTB7: $PC_{71}BM$ were used as active layer. For comparison, a control device with methanol treatment was also fabricated as a reference. The typical current density versus voltage (J–V) characteristics was shown in Figure IV-4 and IV-5. The device performances are summarized in Table IV-2.

The I-PSCs with a methanol treated ZnO performed with a PCE of 7.66 %, a V_{oc} of 0.74 V, a J_{sc} of 14.65 mA/cm^2, and a *FF* of 71.6 %. From Table IV-2 we can see that five interlayers almost delivered the same V_{oc} for the devices. After inserting a thin layer of oligomer electrolytes, the resulting PSCs exhibited enhanced performances, benefiting from the improvements of J_{sc}. The performance **FTF salt** as CIL exhibit more superior than **FBF salt** with a PCE of 7.95 % (V_{oc}= 0.74 V, J_{sc}= 15.12 mA/cm^2, and *FF*= 71.1 %). In another sequence of trimer, fluorinated benzene-fluorene based device, **BfFBf salt**, showed the highest PCE among the oligo-electrolytes which reached 8.26 % with a V_{oc} of 0.74 V, a J_{sc} of 15.72 mA/cm^2, and a *FF* of 71.0 %. The possible reason for **BfFBf salt** have reached the high PCE was the electron withdrawing groups, fluorine, could create the noncovalent

attractive interactions between neighboring moieties and enhancing the self-assembly of the molecules and dipole-dipole interactions.[72-74] **TFT salt** and **BFB salt** gives the good performance too by increasing the PCE more than MeOH-treated ZnO with a PCE 8.17 % (V_{oc}= 0.73 V, J_{sc}= 15.81 mA/cm^2, and *FF*= 70.8 %) for **TFT salt** and 7.98% (V_{oc}= 0.74 V, J_{sc}= 15.17 mA/cm^2, and *FF*= 71.1 %) for **BFB salt**.

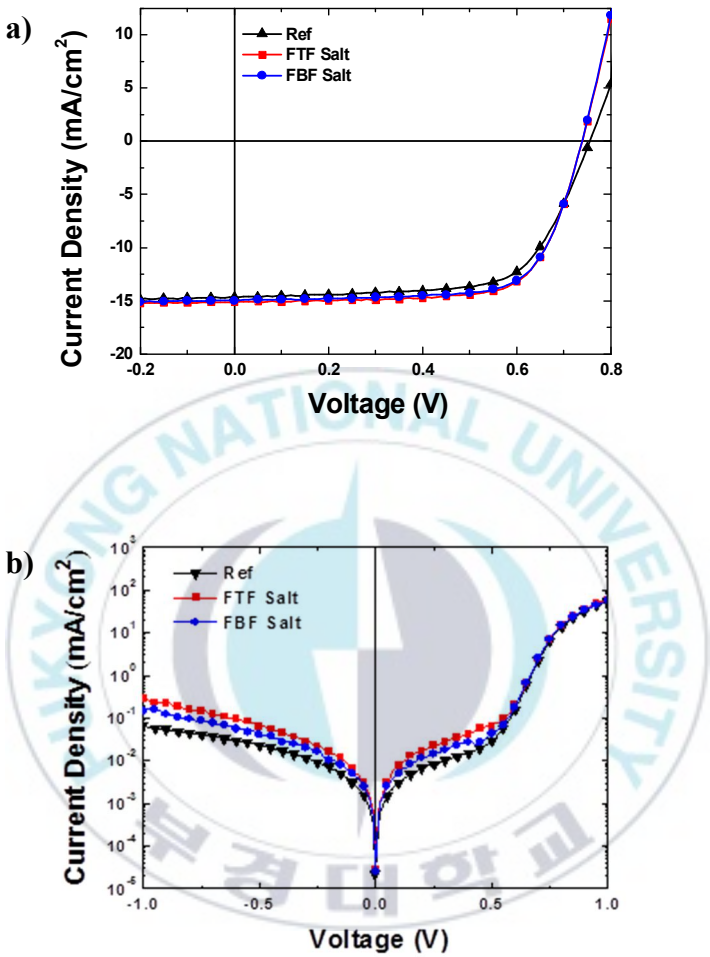

Figure IV-6. Current density–voltage curves of FTF salt and FBF salt as CILs under AM 1.5G (a) simulated illumination with an intensity of 100 mW/cm^2 and under the dark condition (b). The methanol treated ZnO was acted as a reference (ref.).

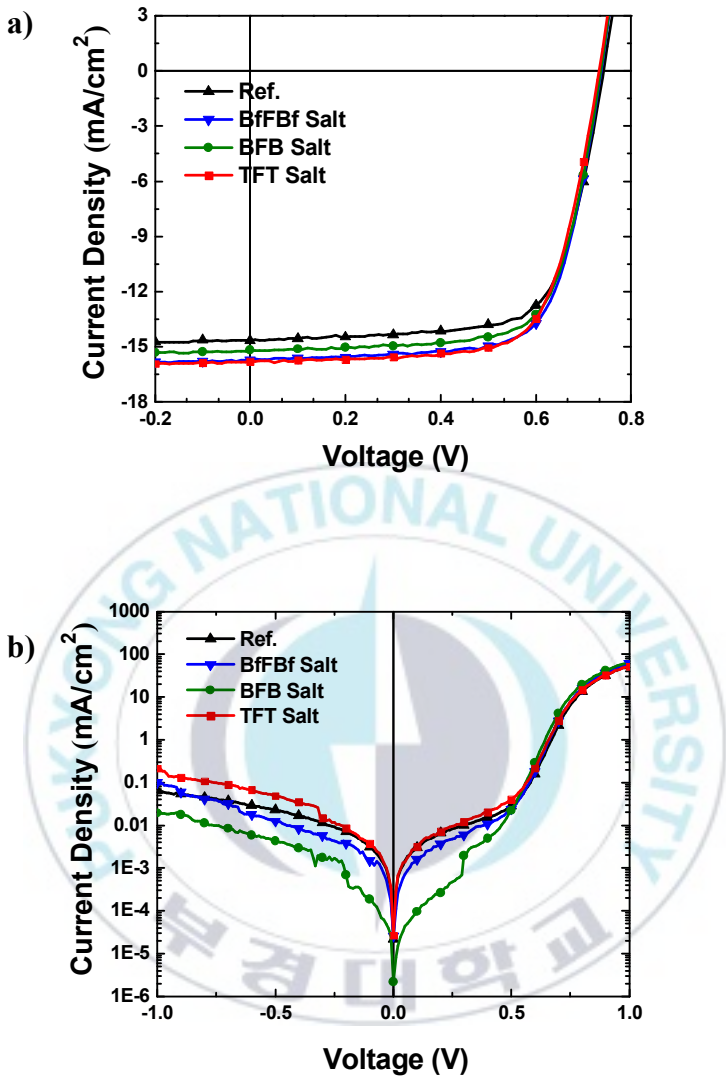

Figure IV-7. Current density–voltage curves of TFT salt, BfFBf salt and BFB salt as CILs under AM 1.5G (a) simulated illumination with an intensity of 100 mW/cm^2 and under the dark condition (b). The methanol treated ZnO was acted as a reference (ref.).

Table IV-2. Summary of the photovoltaic performance of inverted PTB7:$PC_{71}BM$ solar cells with the various interlayer.

Sample Name	Jsc (mA/cm^2)	Voc (V)	FF (%)	PCE (%)
ZnO/MeOH	14.65 (14.55)	0.74 (0.74)	71.6 (71.1)	7.66 (7.66)
ZnO/ FTF Salt	15.12 (15.11)	0.74 (0.74)	71.1 (71.10)	7.95 (7.94)
ZnO/ FBF Salt	14.99(14.97)	0.74 (0.74)	71.1 (70.95)	7.88 (7.85)
ZnO/ BfFBf Salt	15.72(15.22)	0.74 (0.74)	71.0 (71.45)	8.26 (7.99)
ZnO/ BFB Salt	15.17 (14.49)	0.74 (0.74)	71.1 (71.20)	7.98 (7.79)
ZnO/ TFT Salt	15.81 (15.56)	0.73 (0.73)	70.8 (66.3)	8.17 (7.49)

The averages for the photovoltaic parameters of each device are given in parentheses.

IV-4. Conclusion

A series of oligomer electrolytes comprising identical N^+Br^- groups on the side chains but different sequence conjugated main chains fluorene-based small-molecule has synthesized and characterized as cathode interfacial layer. The XPS data was confirmed that the quaternization reaction of all oligomer was succeeded. All oligomer show the absorption in the range of 300-400 nm and have deep HUMO levels which beneficial for blocking the hole from the active layer. The **FTF salt**, **FBF salt**, **TFT salt**, **BFB salt**, **and BfFBf salt** demonstrates a strong impact on the interfacial interaction to the electrode by reducing the work function of ITO. The photovoltaic performances approximately 8.26 % is achieved for OSCs based on a bulk-hetero-junction system consisting of fluorinated benzene-fluorene based device, **BfFBf salt,** as the CIL. **FTF salt**, **FBF salt**, **TFT salt** and **BFB salt** also exhibit a superior performance than MeOH-treated ZnO benefiting from the improvements of $J_{sc.}$

References

[1] B. Dudley, and Team. BP Statistical Review of World Energy. (2016).

[2] D.M. Chapin, C.S. Fuller, G.L. Pearson. (1954), *J. Appl. Phys*., **25**, 676.

[3] H. Spanggaard, F.C. Krebs. (2004), *Solar Energy Materials & Solar Cells.*, **83**, 125–146.

[4] C.J. Brabec, N.S. Sariciftci, J.C. Hummelen. (2001) *Adv. Func. Mater*., **11**, No. 1, 0102-0015-0102-0026.

[5] L. Nian, K. Gao, Liu, F. Kan, Y. Jiang, L. Liu, Z. Xie, X. Peng, T. P. Russell, Y. Ma. (2016), *Adv. Mater*., **28**, 8184−8190.

[6] S. Li, L. Ye, W. Zhao, S. Zhang, S. Mukherjee, H. Ade, J. Hou. (2016), *Adv. Mater*., **28**, 9423−9429.

[7] J. Zhao, Y. Li, G. Yang, K. Jiang, H. Lin, H. Ade, W. Ma, H. Yan. (2016), *Nat. Energy*., **1**, 15027.

[8] J. Huang, J. H. Carpenter, C. Z. Li, J. S. Yu, H. Ade, A. K. Jen. (2016), *Adv. Mater*., **28**, 967−974.

[9] Y. Liu, J. Zhao, Z. Li, C. Mu, W. Ma, H. Hu, K. Jiang, H. Lin, H. Ade, H. Yan. (2014), *Nat. Commun*., **5,** 5293−5300.

[10] W. Zhao, D. Qian, S. Zhang, S. Li, O. Inganas, F. Gao, J. Hou. (2016), *Adv. Mater*., **28**, 4734−4739.

[11] D. Zhu, X. Bao, Q. Zhu, C. Gu, M. Qiu, S. Wen, J. Wang, B. Shahid, R. Yang. (2017), *Energy Environ. Sci.*, **10**, 614.

[12] H. Spanggaard, F.C. Krebs. (2016), *Solar Energy Materials & Solar Cells*, **83**, 125–146.

[13] K.A Vivek and G.D. Agrawal, *IJRET*, **3**.

[14] P. Wurfel. (2007), *Chimia.,* **61**, 770–774.

[15] P.A. Lane and Z.H. Kafafi. (2005), *CRC Press Taylor & Francis Group, Boca Raton, FL*, pp. 49-97.

[16] Z.T. Liu, M.F. Lo, H.B. Wang, T.W. Ng, V.A.L. Roy, C.S. Lee, S.T. Lee. (2009), *Appl. Phys. Lett.*, **95**, 093307-093307-3.

[17] L.S. Roman. (2005), *CRC Press Taylor and Francis Group, Boca Raton, FL.*, 367-384.

[18] L. Zhiqiang, Z. Qifeng, J. Lin, C. Guozhong. (2015), *Energy Environ. Sci*., **8**, 3442-3476.

[19] R. Po, C. Carbonera, A. Bernardi and N. Camaioni. (2011), *Energy Environ. Sci*., **4**, 285–310.

[20] S. Tomoki, U. Tokiyoshi, H. Yuuki, F. Akihiko and Y. Katsumi. (2004), *J. Phys. D: Appl. Phys*., **37**, 847–850.

[21] G. Yu, J. Gao, J. C. Hummelen, F. Wudl and A. J. Heeger. (1995), *Science*, **270**, 1789–1791.

[22] L. Sandro. (2014), *Electronics*, **3**.

[23] R. Xiao, W. Ng Tsz, X. Liang. (2013), *Advanced Materials Research*, **711**, 39-44.

[24] L. Groenendaal, F. Jonas, D. Freitag, H. J. R. Pielartzik, Reynolds. (2000), *Advanced Materials*, **12**, 481–494.

[25] S.A. Carter, M. Angelopoulos, S. Karg, P.J. Brock, J.C. Scott. (1997), *Appl. Phys. Lett.* **70**, 2067–2069.

[26] P. G. Karagiannidis, N. Kalfagiannis, D. Georgiou, A. Laskarakis, N. A. Hastas, C. Pitsalidis, S. Logothetidis. (2012), *J. Mater. Chem*., **22**, 14624–14632.

[27] Y. Xinge, J. M. Tobin, F. Antonio. (2016), *Nature materials*, **15**, 383-396.

[28] R. Bechara, J. Petersen, V. Gernigon, P. Leveque, T. Heiser, V. Toniazzo, D. Ruch, and M. Michel, *Sol. Energy Mater. Sol. Cells*, **98**, 482.

[29] J. Y. Kim, S. Noh, Y. M. Nam, J. Y. Kim, J. Roh, M. Park, J. J. Amsden, D. Y. Yoon, C. Lee, W. H. Jo. (2012), *ACS Appl. Mater. Interfaces*, **3**, 4279–4285.

[30] L.-M. Chen, Z. Xu, Z, Hong, Y. Yang. (2010), *J. Mater. Chem*., **20**, 2575–2598

[31] T. Yang, W. Cai, D. Qin, E. Wang, Li. Lan, X. Gong, J. Peng, Y. Cao. (2010), *J. Phys. Chem. C*, **114**, 6849–6853

[32] K.-S. Shin, H. Jo, H.-J. Shin, W. M. Choi, J.-Y. Choi, S.-W. Kim. (2012), *J. Mater. Chem.*, **22**, 13032

[33] S.-C. Chien, F.-C. Chen, M.-K. Chung, C.-S. Hsu. (2012), *J. Phys. Chem. C*, **116**, 1354–1360.

[34] Nickel F, Reinhard M and Zhang Z. (2012), *Appl. Phys. Lett*. **101**, 053309.

[35] Schulz P, Cowan S and Guan Z. (2014), *Adv. Funct. Mater*., **24**, 701–6.

[36] Yan L, Song Y, Zhou Y, Song B and Li Y. (2015), *Org. Electron*., **17**, 94–101.

[37] Ü. Özgür, Ya. I. Alivov, C. Liu, A. Teke, M. A. Reshchikov, S. Doğan, V. Avrutin, S.-J. Cho, H. Morkoç. (2005), *Journal of Applied Physics*. **98**, 041301.

[38] C.-Y. Li, T.-C. Wen, T.-H. Lee, T.-F. Guo, J.-C.-A. Huang, Y.-C. Lin and Y.-J. Hsu. (2009), *J. Mater. Chem*., **19**, 1643–1647.

[39] S. Woo, W. Hyun Kim, H. Kim, Y. Yi, H.-K. Lyu and Y. Kim. (2014), *Adv. Energy Mater*, **4**, 1301692.

[40] Z. He, C. Zhong, S. Su, M. Xu, H. Wu and Y. Cao. (2012), *Nat.Photonics*, **6**, 591–595.

[41] K. P. Bhuvana, J. Elanchezhiyan, N. Gopalakrishnan and T. Balasubramanian. (2009), *J. Alloys Compd.*, **473**, 534–537.

[42] S. Schumann, R. Da Campo, B. Illy, A. C. Cruickshank, M. A. McLachlan, M. P. Ryan, D. J. Riley, D. W. McComband T. S. Jones. (2011), *J. Mater. Chem*., **21**, 2381–2386.

[43] W. Zihong, S. Chen, C. Yao, etc. (2016), *J. Am. Chem. Soc*. **138**, 2004-201.

[44] Y. Zhou, F. Li, S. Barrau, W. Tian, O. Inganäs, and F. Zhang. (2012), *Sol. Energy Mater. Sol. Cells*, **93**, 497.

[45] F. Zhang, M. Ceder, and O. Inganäs. (2007), *Adv. Mater*. **19**, 1835.

[46] Y. Zhou, C. Fuentes-Hernandez, J. Shim, J. Meyer, A. J. Giordano, H. Li, P. Winget, T. Papadopoulos, H. Cheun, J. Kim, M. Fenoll, A. Dindar, W. Haske, E. Najafabadi, T. M. Khan, H. Sojoudi, S. Barlow, S. Graham, J.-L. Brédas, S. R. Marder, A. Kahn, and B. Kippelen. (2012), *Science*, **336**, 327.

[47] S.-I. Na, T.-S. Kim, S.-H. Oh, J. Kim, S.-S. Kim, and D.-Y. Kim. (2010), *Appl. Phys. Lett.*, **97**, 223305.

[48] S.-I. Na, S.-H. Oh, S.-S. Kim, and D.-Y. Kim. (2009), *Org. Electron.*, **10**, 496.

[49] Y. Ohmori, M. Uchida, K. Muro, K. Yoshino. (1991), *Jpn. J. Appl. Phys.*, **30**, L1941.

[50] M. Grell, D. D. C. Bradley, M. Inbasekaran, E. P. Woo. (1997), *Adv. Mater.*, **9**, 798.

[51] H. Sirringhaus, R. J. Wilson, R. H. Friend, M. Inbasekaran, W. Wu, E. P. Woo, M. Grell, D. D. C. Bradley. (2000), *Appl. Phys. Lett.*, **77**, 406.

[52] D. J. Brennan, P. H. Townsend, D. M. Welsh, M. G. Dibbs, J. M. Shaw, J. L. Miklovich, R. B. Boeke, A. C. Arias, L. Creswell, J. D. MacKenzie, C. Ramsdale, A. Menon, H. Sirringhaus. (2003), *Proc. SPIE*, **5217**, 1.

[53] C. L. Donley, J. Zaumseil, J. W. Andreasen, M. M. Nielsen, H. Sirringhaus, R. H. Friend, J.-S. Kim. (2005), *J. Am. Chem. Soc.*, **127**, 12890.

[54] R. Abbel, A. P. H. J. Schenning, E. W. Meijer. (2008), *Macromolecules*, **41**, 7497.

[55] D. J. D. Moet, M. Lenes, J. D. Kotlarski, S. C. Veenstra, J. Sweelssen, M. M. Koetse, B. de Boer, P. W. M. Blom. (2009), *Org. Electron.*, **10**, 1275.

[56] M. Grell, D. D. C. Bradley, G. Unggar, J. Hill, K.S. Whitehead. (1999), *Macromolecules*, **32**, 5810.

[57] G. Lieser, M. Oda, T. Miteva, A. Meisel, H.-G. Nothofer, U. Scherf, D. Neher. (2000), *Macromolecules*, **33**, 4490.

[58] J. Luo, H. B. Wu, C. He, A. Y. Li, W. Yang, Y. Cao. (2009), *Appl. Phys. Lett.*, **95**, 043301.

[59] Smith, Michael March, Jerry. (2001), *Advanced Organic Chemistry: Reactions, Mechanisms, and Structure,* **5**th ed., New York, NY: Wiley-Interscience.

[60] X. Jin, He. Yunping, L. Chao, F. Wu, Y. Xu, L. Huang, L. Chen, and Y. Chen. (2016), *Solar Energy Materials & Solar Cells*, **157**, 644–651.

[61] E. Zhou, K. Tajima, C. Yang and K. Hashimoto. (2010), *J. Mater. Chem*., **20**, 2362–2368.

[62] Y. Li, Y. Cao, J. Gao, D. Wang, G. Yu, A. J. Heeger. (1999), *Synth. Met*., **99**, 243.

[63] Y. Liu, Z. A. Page, T. P. Russell and T. Emrick. (2015), *Angew. Chem., Int. Ed.*, **54**, 11485–11489.

[64] B. R. Lee, E. D. Jung, Y. S. Nam, M. Jung, J. S. Park, et. al. (2014), *Adv. Mater*., **26**, 494–500.

[65] P. Fu, X. Guo, S. Wang, Y. Ye and C. Li. (2017), *Appl. Mater. Interfaces*, **9**, 13390-13395.

[66] S.-H. Liao, Y.-L. Li, T.-H. Jen, Y.-S. Cheng, S.-A.Chen. (2012), *J. Am. Chem. Soc*. **134**, 14271.

[67] Z. Liang, Q. Zhang, L. Jiang and G. Cao. (2016), *Energy Environ. Sci.,* **8**, 3442-3476.

[68] S. van Reenen, S. Kouijzer, R. A. J. Janssen, M. M. Wienk and M. Kemerink. (2014), *Adv. Mater. Interfaces,* **1**, 1400189.

[69] F. Huang, Y. Zhang, M. S. Liu, A. K. Y. Jen. (2009), *Adv. Funct. Mater*., **19**, 2457-2466.

[70] J. H. Seo, T. Q. Nguyen. (2008), *J. Am. Chem. Soc*., **130**, 10042- 10043.

[71] Y. Wang, S. R. Parkin, J. Gierschner, M. D. Watson. (2008), *Org. Lett*., **10**, 3307- 3310.

[72] F. Babudri, G. M. Farinola, F. Naso, R. Ragni. (2007), *Chem. Commun*., **10**, 1003-1022.

[73] K. Reichenbacher, H. I. Suss, J. Hulliger. (2005), *Chem. Soc. Rev*., **34**, 22-30.

Acknowledgement

Thanks to merciful Lord, Allah SWT for all the countless gifts that have offered me which can strengthen me until I finished this study.

I am grateful to my advisor, Professor Joo Hyun Kim whose expertise, understanding, generous guidance and his support made it possible for me to study and did the research on a fascinating topic that will be useful for my future.

I would like to thank my fellow labmates in Organic Optoelectronic Materials Lab (OOM): Nadhila S., Y.H. Kim, D.G. Kim, and H.C. Jin. Their help, care, and encouragement have been especially valuable to pursue the success of my thesis. They gave me a comfortable and good work environment for last two years. I also would like to thank to all my Indonesian friends in Pukyong National University especially Nurmaulia, Sabrina, Sella, Nurul, Yosia, Zeno, Aldias, Fajar and so many that I grateful to have them in Korea. They have supported me throughout entire process, both by keeping me harmonious and helping me putting pieces together. I will be grateful forever for our friendship.

I am grateful to all professors in Department of Polymer Engineering especially: B. Lee, S.I. Yoo, M.H. Kim, and U.H. Choi, for knowledge, encouragement and comprehensive advice until this work came to existence. I am thankful to all my professors at the Department of Chemical Engineering in Diponegoro University, who provided many engineering tools and basic knowledge that I gained in their class. And I also would like to thank all officers at Department of Polymer Engineering who always help me to comply with all of the necessary formalities during my study.

I would like to express my extreme sincere gratitude to my beloved parents and family who always pray for me and proud of me. Their support launched the greater part of the sustainability my life in this overseas country.

Mutia Anissa Marsya